NACA RM No. L8I08

NACA

RESEARCH MEMORANDUM

LONGITUDINAL-STABILITY INVESTIGATION OF HIGH-LIFT AND STALL-CONTROL DEVICES ON A 52° SWEPTBACK WING WITH AND WITHOUT FUSELAGE AND HORIZONTAL TAIL AT A REYNOLDS NUMBER OF 6.8×10^6

By

Gerald V. Foster and James E. Fitzpatrick

Langley Aeronautical Laboratory
Langley Field, Va.

NATIONAL ADVISORY COMMITTEE
FOR AERONAUTICS
WASHINGTON

December 20, 1948
Declassified September 15, 1955

NACA RM No. L8I08

NATIONAL ADVISORY COMMITTEE FOR AERONAUTICS

RESEARCH MEMORANDUM

LONGITUDINAL-STABILITY INVESTIGATION OF HIGH-LIFT AND STALL-CONTROL DEVICES ON A 52° SWEPTBACK WING WITH AND WITHOUT FUSELAGE AND HORIZONTAL TAIL AT A REYNOLDS NUMBER OF 6.8×10^6

By Gerald V. Foster and James E. Fitzpatrick

SUMMARY

An investigation has been conducted in the Langley 19-foot pressure tunnel to determine the separate and combined effects of high-lift and stall-control devices, a fuselage, and the vertical position of a swept-back horizontal tail on the aerodynamic characteristics of a 52° swept-back wing. The wing had an aspect ratio 2.88, taper ratio 0.625, and NACA 64_1-112 airfoil sections normal to the 0.282-chord line. The high-lift and stall-control devices consisted of split flaps, leading-edge flaps, and upper-surface fences. These test data were obtained at a Reynolds number of 6.8×10^6 which corresponded to a Mach number of 0.13.

The results of the investigation indicate that the increase in maximum lift of the wing with leading-edge and trailing-edge flaps was slightly larger than the sum of the lift increments contributed individually by the flaps. The stability of the wing in the moderate lift-coefficient range (0.7 to 0.9) was decreased with leading-edge flaps and beyond this lift-coefficient range the wing stall spread outboard resulting in further decrease in stability. The tip stall and resulting unstable pitching moment which occurred with leading-edge flaps on the wing were improved with upper-surface fences. Upper-surface fences caused the pitching-moment curve of the wing with $0.575\frac{b}{2}$-span leading-edge flaps and split flaps to break in a stable direction at the maximum lift.

The fuselage decreased the stability of the stable wing configuration; whereas, the fuselage had negligible effect on the stability of the unstable configurations.

The horizontal tail increased the stability of the wing-fuselage combination in the linear lift range; however, the increase in stability decreased as the position of the tail was lowered. In the nonlinear

lift range, the high tail position contributed a destabilizing effect while most configurations indicated an increase in stability with the tail in the low position.

INTRODUCTION

Means of counteracting the inherent disadvantages associated with swept wings operating at low speeds are being investigated in the Langley 19-foot pressure tunnel (references 1 to 4). As a part of this investigation, tests have been made to determine the longitudinal stability and yaw characteristics at large values of Reynolds number of a 52° sweptback wing of aspect ratio 2.88, taper ratio 0.625, and NACA 64_1-112 airfoil sections perpendicular to the 0.282-chord line. The longitudinal stability characteristics of the wing with and without split flaps have been presented in reference 5 and the yaw characteristics have been presented in reference 6.

The present paper contains the results of the longitudinal stability investigation concerned with the separate and combined effects of high-lift and stall-control devices, a fuselage, and the vertical position of a sweptback horizontal tail. The high-lift and stall-control devices consisted of split flaps, leading-edge flaps, and upper-surface fences. The fuselage was tested in a low-wing and midwing position. The tail was tested at various vertical locations for both wing-fuselage combinations. The data presented herein were obtained at a Reynolds number of 6.8×10^6 which corresponded to a Mach number of 0.13.

SYMBOLS

C_L	lift coefficient (Lift/qS)
C_D	drag coefficient (Drag/qS)
C_m	pitching-moment coefficient; moment about the quarter chord of mean aerodynamic chord (Moment/qS$\bar{c}$)
α	angle of attack of wing chord, degrees
S	wing area, square feet
b	wing span, feet

$\bar{c}$ mean aerodynamic chord measured parallel to the plane of symmetry, feet $\left(\frac{2}{S}\int_0^{b/2} c^2\,dy\right)$

c local chord measured parallel to the plane of symmetry, feet

y spanwise distance from plane of symmetry, feet

q free-stream dynamic pressure, pounds per square foot $\left(\frac{1}{2}\rho V^2\right)$

ρ mass density of air, slugs per cubic foot

V free-stream velocity, feet per second

ϵ effective downwash angle, degrees

q_t/q ratio of effective dynamic pressure at the tail to free-stream dynamic pressure

i_t incidence of horizontal tail with respect to wing chord plane, degrees

h perpendicular distance between the wing chord plane extended and the tail $0.25\bar{c}$ point

$\left(C_{m_{i_t}}\right)_0$ effectiveness of horizontal tail on wing-fuselage combination at $C_L = 0$

Δi_t angular difference between the two incidences of horizontal tail used

MODEL

The general arrangements for the wing equipped with leading-edge flaps, split flaps, upper-surface fences, fuselage, and a horizontal tail are presented in figures 1 and 2.

The wing had 52.05° sweepback at the leading edge and NACA 64_1-112 airfoil sections normal to the 0.282-chord line of the wing. The aspect ratio and taper ratio of the wing were 2.88 and 0.625, respectively. The wing had no twist or dihedral.

The constant-chord leading-edge flaps were investigated with spans of $0.575\frac{b}{2}$ and $0.725\frac{b}{2}$. The outboard ends of these flaps were located at 0.975 percent of the wing semispan. The angle of the flap chord with respect to the wing chord amounted to 50° measured in a plane normal to the 0.282-wing-chord line.

The split flaps, measured in a plane perpendicular to the 0.282-chord line, had a chord equal to 20 percent of the local wing chord and were deflected 60° from the wing lower surface. The span of these flaps extended outboard $0.50\frac{b}{2}$ from the plane of symmetry for the plain wing and low-wing-fuselage combination. With the midwing fuselage configuration a section of the flaps (30 percent of the flap span) was removed to allow for the fuselage.

The upper-surface fences were of a constant height of 60 percent of the maximum local airfoil thickness and extended over 95 percent of the airfoil chord measured from the trailing edge.

The circular fuselage had a maximum diameter of 34.8 percent of the root chord and a fineness ratio of 10.2. The profile of the fuselage is defined in reference 1. Two wing positions relative to the fuselage center line were tested. For a low-wing position, the 28.2-percent wing-chord line was 37.8 percent of the maximum fuselage diameter below the fuselage center line. With the midwing fuselage combination, the 28.2-percent wing-chord line was located on the fuselage center line. Fillets were not used at the wing-fuselage junctures. A positive incidence of 2° existed between the wing-chord plane and the fuselage center line.

The horizontal tail used during these tests had 42.05° sweepback at the leading edge, an aspect ratio of 4.01, a taper ratio of 0.625, and NACA 0012-64 airfoil sections parallel to the plane of symmetry. The vertical location of the tail is defined as the perpendicular distance between the wing-chord plane extended and the tail $0.25\bar{c}$ point (see fig. 2) and was adjustable by means of the strut to which the tail was attached. The incidence of the tail is referred to the wing-chord plane and was changed by rotation about a line through the $0.25\bar{c}$ of the tail.

TESTS AND CORRECTIONS

Tests

All tests were conducted with the air in the tunnel compressed to an absolute pressure of approximately 33 pounds per square inch. Based on the wing mean aerodynamic chord, the Reynolds number of the tests

was 6.8×10^6 which corresponded to a Mach number of 0.13. Figure 3 shows one of the wing–fuselage combinations mounted in the tunnel.

Measurements of the aerodynamic forces and moments were obtained through an angle–of–attack range from -4° to 28°, except for the midwing–fuselage combination and some wing–fuselage combinations with the horizontal tail where the maximum angle of attack was 1° or 2° lower. In addition, visual observations of the stall were obtained for several model configurations by means of tufts attached to the upper surface of the wing.

Tables I, II, and III may be used as a guide to the various arrangements of wing, flaps, and tail tested.

Corrections

The test data are presented in nondimensional coefficient form and have been corrected for the effects of the tare and interference of model supports and air–stream misalinement. Jet–boundary corrections based on the method presented in reference 7 have been applied to the angle of attack and drag coefficient. The pitching–moment coefficients have been corrected for the distortion of the wing loading induced by the tunnel.

RESULTS AND DISCUSSION

Wing Configurations

Leading–edge flaps and split flaps.– The effect of the leading–edge flaps on several aerodynamic characteristics of the wing with and without split flaps are shown in figure 4. The more important results of these data have been summarized in table I.

The values of maximum lift coefficient presented in table I indicate that the sum of the increments of maximum lift contributed by the split flaps and leading–edge flaps (based on plain wing) considerably underestimated the increment of maximum lift obtained when the wing was tested with both flaps deflected simultaneously. Slightly higher values of maximum lift were obtained on a 42° sweptback wing equipped with similar flaps (reference 1), and the sum of the individual increments of maximum lift slightly overestimated the increment obtained from the combination.

It can be seen from figures 4(a) and 4(b) that for the wing without leading–edge flaps with or without split flaps deflected a marked increase in stability is obtained through the lift range up to a C_L of about 0.9. This increase in stability is associated with a rearward movement of center of pressure which could be attributed, as pointed out in reference 5,

to small increases in lift near the tip caused by the action of the vortex flow over the outer portion of the wing. A further increase in angle of attack resulted in complete separation of flow at the tip (fig. 5) and accompanying instability.

When the leading-edge flaps were deflected, the stability in the lift range up to a C_L of about 0.9 was decreased (figs. 4 and 5). It can be seen in figure 6 that through the linear lift range the additions of leading-edge flaps resulted in forward shifts of the aerodynamic center up to 5 percent of the mean aerodynamic chord. The decrease in stability in the low lift range (C_L up to 0.7) is attributed to the unstable moment contributed by the leading-edge flaps and in the moderate lift range ($C_L = 0.7$ to $C_L = 0.9$) to the inability of the leading-edge vortex to form with the leading-edge flap present. Although the leading-edge flaps caused the initial stall to occur at the inboard end of the flap, the stall spread outboard with the result that instability was obtained at maximum lift. A previous investigation of a 42° sweptback wing indicated similiar decreases in stability in the low and moderate lift range with the addition of leading-edge flaps (reference 2). With either the $0.575\frac{b}{2}$-span or the $0.725\frac{b}{2}$-span leading-edge flap, stall studies of the 42° sweptback wing indicated that the stall also began at the inboard end of the flap but it spread inboard more rapidly than it spread outboard, thereby effecting a stable break in the pitching-moment curves (reference 1).

Upper-surface fences.- The effects of upper-surface fences on the aerodynamic characteristics of several model configurations have been briefly investigated and the results are presented in figures 7 to 9. It was found that fences placed separately at spanwise location of $0.30\frac{b}{2}$-span and $0.45\frac{b}{2}$-span stations had a negligible effect on the aerodynamic characteristics of the plain wing and therefore have not been presented.

The results obtained with the $0.575\frac{b}{2}$-span leading-edge flaps indicate that fences located $0.05\frac{b}{2}$ outboard of the inboard end of the flaps ($0.45\frac{b}{2}$-spanwise station) delayed tip stall and produced a stable pitching-moment slope to just below $C_{L_{max}}$ (fig. 7). When split flaps were deflected the stability was decreased slightly in the high-lift range prior to $C_{L_{max}}$, beyond which however the pitching-moment curve broke in a stable direction. Although the angle of attack was increased approximately 5° beyond that at which the pitching-moment curve broke stable with only a very small reduction in $C_{L_{max}}$, it is believed that further increase of angle of attack would result in an unstable condition.

Two spanwise positions of the fence were tested in conjunction with the $0.725\frac{b}{2}$-span leading-edge flaps and split flaps (fig. 8). Although the results are not as favorable as those for the $0.575\frac{b}{2}$-span leading-edge flaps, there was an improvement in stability prior to $C_{L_{max}}$; however, at or near $C_{L_{max}}$, the moment curves broke in an unstable direction. It can be seen in figure 9 that the tip stall is delayed but not as effectively as for the short-span leading-edge flap.

Wing-Fuselage Configurations

Several wing configurations were tested in conjunction with a fuselage (figs. 10 to 14) in a low-wing position and midwing position. The results of these tests have been summarized in table II. No fillets were used at the wing-fuselage junctions for either configuration and therefore local effects at the junctures may be severe.

The fuselage in the low-wing position caused very small changes in lift throughout the angle-of-attack range for either the plain-wing or flapped-wing configuration. The fuselage in the midwing position had little effect on the lift of the plain wing but it did result in lower values of lift prior to $C_{L_{max}}$ for the configurations with split flaps deflected. The reduction in lift is due to the removal of 30 percent of the split-flap span to allow for the intersection of the fuselage. It is of interest to note, however, that even with the center portion of the split flaps removed the values of maximum lift obtained with the midwing position were equal to or slightly greater than those obtained for either the flapped wing alone or low-wing position. It is believed that the juncture of the midwing configuration is more favorable than that of the low-wing position, although the reason for the increase in lift over that obtained with the wing with the fuselage off is not readily apparent.

The data shown in figure 10(a) for the unflapped wing indicate that the drag increase due to the fuselage is very small and is relatively independent of wing position. For the flap-deflected configurations (figs. 10(b), 11, and 13), an appreciable increase in drag attributable to the fuselage for the low-wing position occurred, whereas for the mid-wing position the results indicate a drag variation comparable to that of the fuselage-off configuration with split flaps.

In the linear lift range the fuselage caused a slight rearward shift in center of pressure and a small decrease in stability of the unflapped wing (fig. 10(a)). When the split flaps were deflected, the results for the midwing position show a relatively large rearward shift in center of pressure which can be attributed to the removal of the center portion of the split flaps (figs. 10(b) and 11). The effect of the fuselage on the

location of the aerodynamic center is presented in figure 12 and indicates that the fuselage caused a small forward shift in the aerodynamic center in the low and moderate lift ranges. The stability prior to and at $C_{L_{max}}$ was little affected by the presence of the fuselage for all configurations except when the flaps were deflected and fences were added. The data for the flaps-deflected configuration with fences (fig. 13) indicate, at or near $C_{L_{max}}$, the stability of the wing was reduced with the addition of the fuselage. A comparison of the stall patterns (figs. 9 and 14) does not provide an explanation for the change in direction of pitching-moment break although this may be due to an inability to recognize small shifts in center of pressure by tuft observation. Even though the fences with the fuselage present did not provide the stability obtained without the fuselage, they did improve the stability up to $C_{L_{max}}$ (compare figs. 11 and 13).

The results of tests of other fence locations and combinations are presented in table II. A combination of fences located at $0.30\frac{b}{2}$-span and $0.45\frac{b}{2}$-span stations or 10 percent farther outboard had a negligible effect on the stability in the high lift range.

Wing-Fuselage-Tail Configurations

The effect of a tail, located at several vertical positions, on the lift and pitching-moment characteristics of various wing-fuselage combinations is presented in figures 15 and 16. The data presented are for only one of the two tail incidences tested. A summary of the pitching-moment characteristics is presented in table III. Variations of effective downwash and dynamic-pressure ratio have been included in these figures. The values of effective downwash were determined from pitching-moment data with tail on and tail off. The values of effective dynamic-pressure ratio were determined from the tail effectiveness obtained from tail-on tests and are based on values of $\left(C_{m_{i_t}}\right)_0$ at zero lift (table IV). The slope of the downwash curves through the linear lift range is also presented in table IV.

Linear lift range.- The strong influence of the fuselage on the effective downwash can be seen by an inspection of the downwash curves in the vicinity of zero lift (fig. 15). The tail in a position below the fuselage is operating in an effective upwash of approximately 2° while the tail in a position just above the fuselage is operating in an effective downwash of 2°. Even for the highest tail positions $\left(\text{that is, } 0.50\frac{h}{b/2}\right)$ the influence of the sharp afterbody of the fuselage is pronounced.

Comparing the stability obtained with the tail on to that obtained with the tail off, the results indicate that through the linear lift range the stability (as measured by $dC_m/d\alpha$) was greatly increased by the presence of the tail. The increase in stability decreased at each successively lower tail position (table III and fig. 17). As the tail was moved from the high to low position, the aerodynamic-center location was moved forward as much as 7 percent of mean aerodynamic chord. Inasmuch as there is a negligible variation of q_t/q through the angle-of-attack range for all tail positions tested, the change in stability between the various tail positions can be associated with the increased values of $d\epsilon/d\alpha$ for the low tail positions (table IV). These results are, in general, comparable to those obtained in a similar investigation with a 42° sweptback wing (reference 8) and also to those obtained from surveys behind a 42° sweptback wing (reference 9).

Nonlinear lift range.- At high lift coefficients the tail in the high position was operating in a field of greatly increased $d\epsilon/d\alpha$ and was becoming enveloped in a wake with the result that the tail actually contributed a destabilizing effect (figs. 15 and 16). The stability contributed by the tail in the low position was in most cases increased in the nonlinear lift range over that in the linear lift range because of the reduced values of $d\epsilon/d\alpha$ and the reduced effects of q_t/q.

The stability contributed by the tail was not appreciably altered when the flaps were deflected (fig. 15). The differences in stability are confined to the differences obtained for the tail-off configurations.

The results indicate that the tail in a position below the fuselage gave the most desirable increase in stability throughout the lift range. It should be mentioned, however, that a fuselage afterbody having a more gradual taper and an improved fuselage-wing juncture might increase the effectiveness of the tail in the high positions.

In general, the stabilizing effectiveness of the tail is approximately the same for the present wing and the 42° sweptback wing of reference 8; however, the complete configurations for the 42° sweptback are more satisfactory because of the greater stability of the wing-fuselage combinations.

CONCLUDING REMARKS

The results of a longitudinal-stability investigation of a 52° sweptback wing tested in various combinations with high-lift and

stall-control devices, a fuselage, and a sweptback horizontal tail indicate that:

1. The increase in maximum lift of the wing attained with leading-edge and trailing-edge flaps in combination was slightly larger than the sum of the lift increments contributed individually by the flaps.

2. The addition of leading-edge flaps to the plain wing or to the wing with split flaps caused a decrease in stability in the moderate lift-coefficient range (0.7 to 0.9). Beyond this lift-coefficient range the wing stall spreads outboard, resulting in further decrease in stability.

3. Upper-surface fences with leading-edge flaps delayed the tip stall and produced a stable pitching-moment slope to just below the maximum lift coefficient. Fences caused the pitching-moment curve of the wing with $0.575\frac{b}{2}$-span leading-edge flaps and split flaps to break in a stable direction at the maximum lift coefficient.

4. The fuselage decreased the stability of the stable wing configuration; however, it had a negligible effect on the unstable wing configurations.

5. The horizontal tail increased the stability of the wing-fuselage combination in the linear lift range; however, the increase in stability decreased as the position of the tail was lowered. In the nonlinear lift range, the high tail position contributed a destabilizing effect while most configurations indicated an increase in stability with the tail in the low position.

Langley Aeronautical Laboratory
National Advisory Committee for Aeronautics
Langley Field, Va.

REFERENCES

1. Graham, Robert R., and Conner, D. William: Investigation of High-Lift and Stall-Control Devices on an NACA 64-Series 42° Sweptback Wing with and without Fuselage. NACA RM No. L7G09, 1947.

2. Conner, D. William, and Neely, Robert H.: Effects of a Fuselage and Various High-Lift and Stall-Control Flaps on Aerodynamic Characteristics in Pitch of an NACA 64-Series 40° Swept-Back Wing. NACA RM No. L6L27, 1947.

3. Neely, Robert H., and Koven, William: Low-Speed Characteristics in Pitch of a 42° Sweptback Wing with Aspect Ratio 3.9 and Circular-Arc Airfoil Sections. NACA RM No. L7E23, 1947.

4. Koven, William, and Graham, Robert R.: Wind-Tunnel Investigation of High-Lift and Stall-Control Devices on a 37° Sweptback Wing of Aspect Ratio 6 at High Reynolds Numbers. NACA RM No. L8D29, 1948.

5. Fitzpatrick, James E., and Foster, Gerald V.: Static Longitudinal Aerodynamic Characteristics of a 52° Sweptback Wing of Aspect Ratio 2.88 at Reynolds Numbers from 2,000,000 to 11,000,000. NACA RM No. L8H25, 1948.

6. Salmi, Reino J.: Yaw Characteristics of a 52° Sweptback Wing NACA 64_1-112 Section with a Fuselage and with Leading-Edge and Split Flaps at Reynolds Numbers from 1.93×10^6 to 6.00×10^6. NACA RM No. L8H12, 1948.

7. Eisenstadt, Bertram J.: Boundary-Induced Upwash for Yawed and Swept-Back Wings in Closed Circular Wind Tunnels. NACA TN No. 1265, 1947.

8. Spooner, Stanley H., and Martina, Albert P.: Longitudinal Stability Characteristics of a 42° Sweptback Wing and Tail Combination at a Reynolds Number of 6.8×10^6. NACA RM No. L8E12, 1948.

9. Furlong, G. Chester, and Bollech, Thomas V.: Downwash, Sidewash, and Wake Surveys behind a 42° Sweptback Wing at a Reynolds Number of 6.8×10^6 with and without a Simulated Ground. NACA RM No. L8G22, 1948.

TABLE I.- SUMMARY OF AERODYNAMIC CHARACTERISTICS OF A 52° SWEPTBACK WING WITH AND WITHOUT VARIOUS HIGH-LIFT AND STALL-CONTROL DEVICES

Configuration	Span of L.E. flap (b/2)	$C_{L_{max}}$	α at $C_{L_{max}}$	D/L at 0.85 $C_{L_{max}}$	C_m-characteristics	Type of C_L-peak	Fig. no.
	off	1.12	27.1	0.190	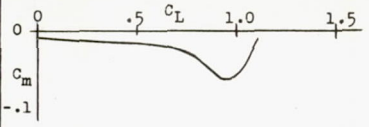		4(a)
	.725	1.24	[a]28.2	.189	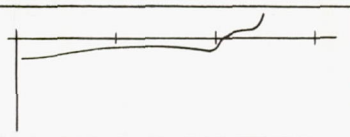		4(a)
	.575	1.17	[a]28.2	.195	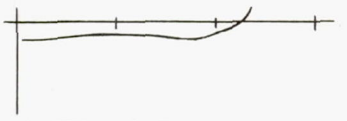		4(a)
	.725	1.36	27.0	.184	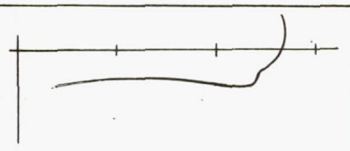		4(b)
	.575	1.32	27.3	.194	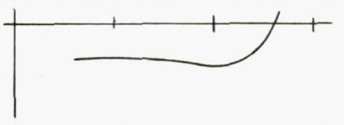		4(b)
	off	1.15	22.1	.165	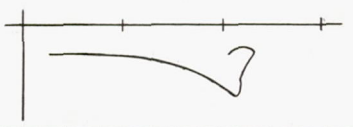		4(b)
 Fences at 0.45b/2	.575	1.10	[a]28.2	.157	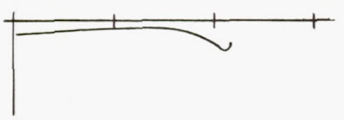		7
 Fences at 0.45b/2	.575	1.27	24.0	.176	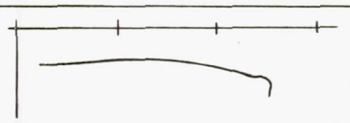		7
 Fences at 0.30b/2	.725	1.41	26.4	.189	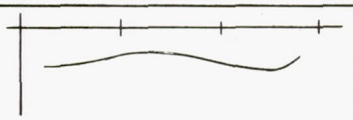		8
 Fences at 0.45b/2	.725	1.35	26.5	.182			8

[a]Maximum angle of attack tested.

TABLE II.- SUMMARY OF AERODYNAMIC CHARACTERISTICS OF A 52° SWEPTBACK WING WITH FUSELAGE AND VARIOUS HIGH-LIFT AND STALL-CONTROL DEVICES

Configuration	Fuselage position	Span of L.E. flaps (b/2)	$C_{L_{max}}$	α at $C_{L_{max}}$	D/L at 0.85 $C_{L_{max}}$	C_m-characteristics	Type of C_L-peak	Fig. no.
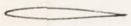	Mid	Off	1.17	26.6	0.223	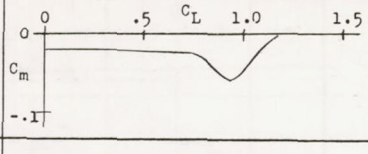		10(a)
	Low	Off	1.14	26.0	.203	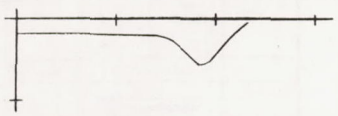		10(a)
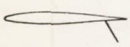	Mid	Off	1.17	24.0	.170	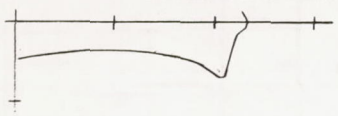		10(b)
	Low	Off	1.10	21.7	.164	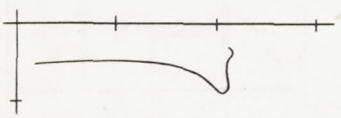		10(b)
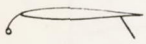	Mid	.575	1.34	26.8	.210	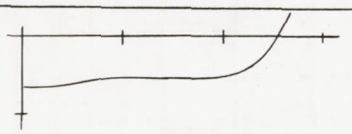		11
	Low	.575	1.31	26.3	.197	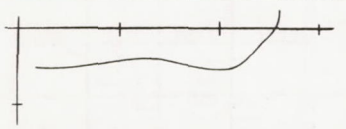		11
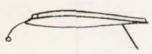 Fences at 0.45b/2	Mid	.575	1.39	[a]27.4	.213	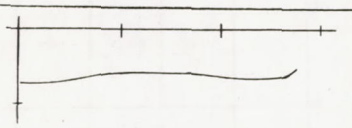		13
	Low	.575	1.31	24.3	.191	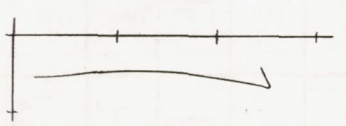		13
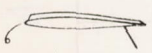 Fences at 0.30b/2 and 0.45b/2	Low	.575	1.24	21.3	.185	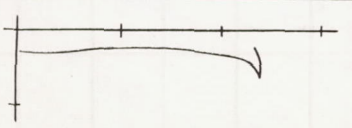		-----
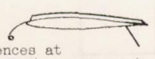 Fences at 0.40b/2 and 0.55b/2	Low	.575	1.22	21.7	.188	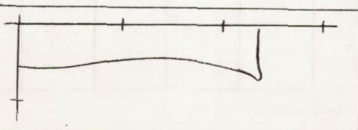		----

[a]Maximum angle of attack tested.

NACA

TABLE III.- SUMMARY OF PITCHING-MOMENT CHARACTERISTICS OF A 52° SWEPTBACK WING IN COMBINATION WITH A FUSELAGE AND HORIZONTAL TAIL

Configuration		Tail height, percent b/2 above chord plane extended	C_m-characteristics
Flap	Wing		
Off	Mid	Tail off	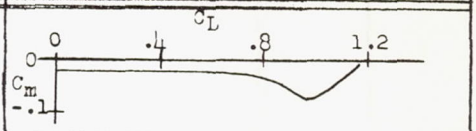
		50.2	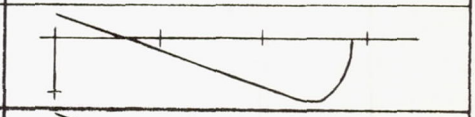
		37.2	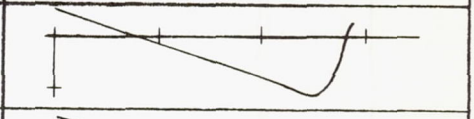
		19.6	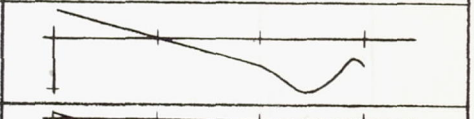
		-7.4	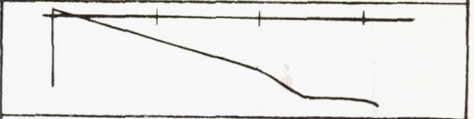
$0.575\frac{b}{2}$ span L.E. flap, Split flap, and fences at $0.45\frac{b}{2}$	Mid	Tail off	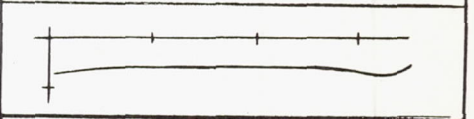
		50.2	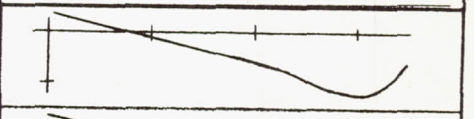
		37.2	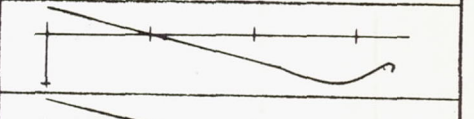
		19.6	
		-7.4	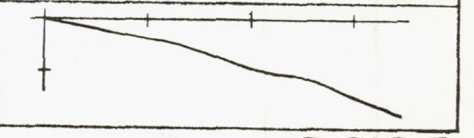

NACA

TABLE III.- SUMMARY OF PITCHING-MOMENT CHARACTERISTICS OF A 52° SWEPTBACK WING IN COMBINATION WITH A FUSELAGE AND HORIZONTAL TAIL - Concluded

Configuration		Tail height, percent b/2 above chord plane extended	C_m-characteristics
Flap	Wing		
Off	Low	Tail off	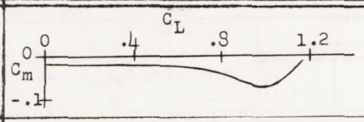
		61.5	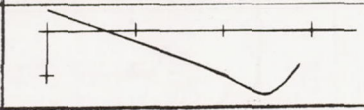
		48.3	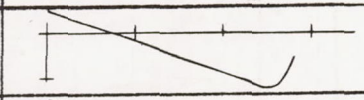
		30.7	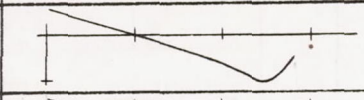
		3.7	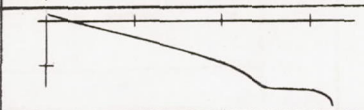
$0.575\frac{b}{2}$-span L.E. flap and split flap	Low	Tail off	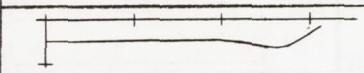
		61.5	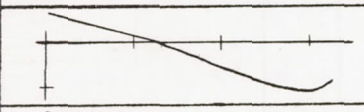
		30.7	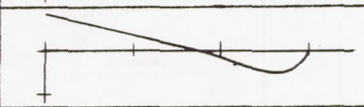
		3.7	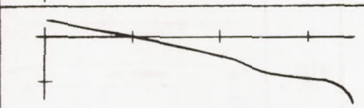
$0.575\frac{b}{2}$-span L.E. flap, split flap, and fences at $0.45\frac{b}{2}$	Low	Tail off	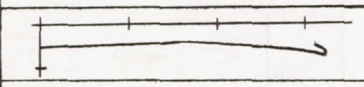
		61.5	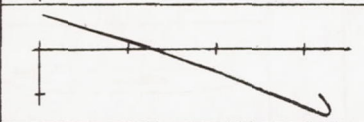
		48.3	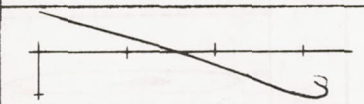
		30.7	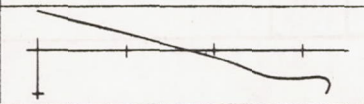
		3.7	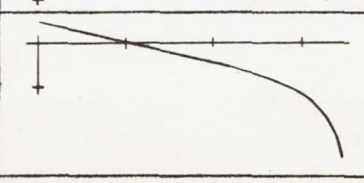

TABLE IV.- MEASURED VALUES OF $d\epsilon/d\alpha$ IN THE LINEAR LIFT RANGE

Configuration			$\left(C_{m_{i_t}}\right)_0$	Δi_t (deg)	$d\epsilon/d\alpha$
Fuselage	Flaps	Position of tail (2h/b)			
Midwing	Off	0.502	0.0153	3.6	0.36 increasing to 0.51
		.372	.0147	3.6	.51
		.196	.0153	3.8	.51 increasing to .65
		−.074	.0125	4.4	.52
	0.575$\frac{b}{2}$-span L.E. flaps, split flaps, and fences	.502	.0155	3.6	.41 increasing to .50
		.372	.0159	3.4	.50
		.196	.0158	3.6	.51 increasing to .62
		−.074	.0130	4.0	.55 decreasing to .47
Low-wing	Off	.615	.0158	3.6	.43
		.483	.0152	3.5	.42
		.307	.0156	3.6	.53
		.037	.0153	3.6	.60
	0.575$\frac{b}{2}$-span L.E. flaps and split flaps	.615	.0134	3.8	.36
		.483	------	---	----------
		.307	.0138	4.0	.36 increasing to .68
		.037	.0130	4.3	.57
	0.575$\frac{b}{2}$-span L.E. flaps, split flaps, and fences	.615	.0132	4.1	.37
		.483	.0146	3.9	.46
		.307	.0144	3.9	.43 increasing to .55
		.037	.0141	4.1	.62

NACA

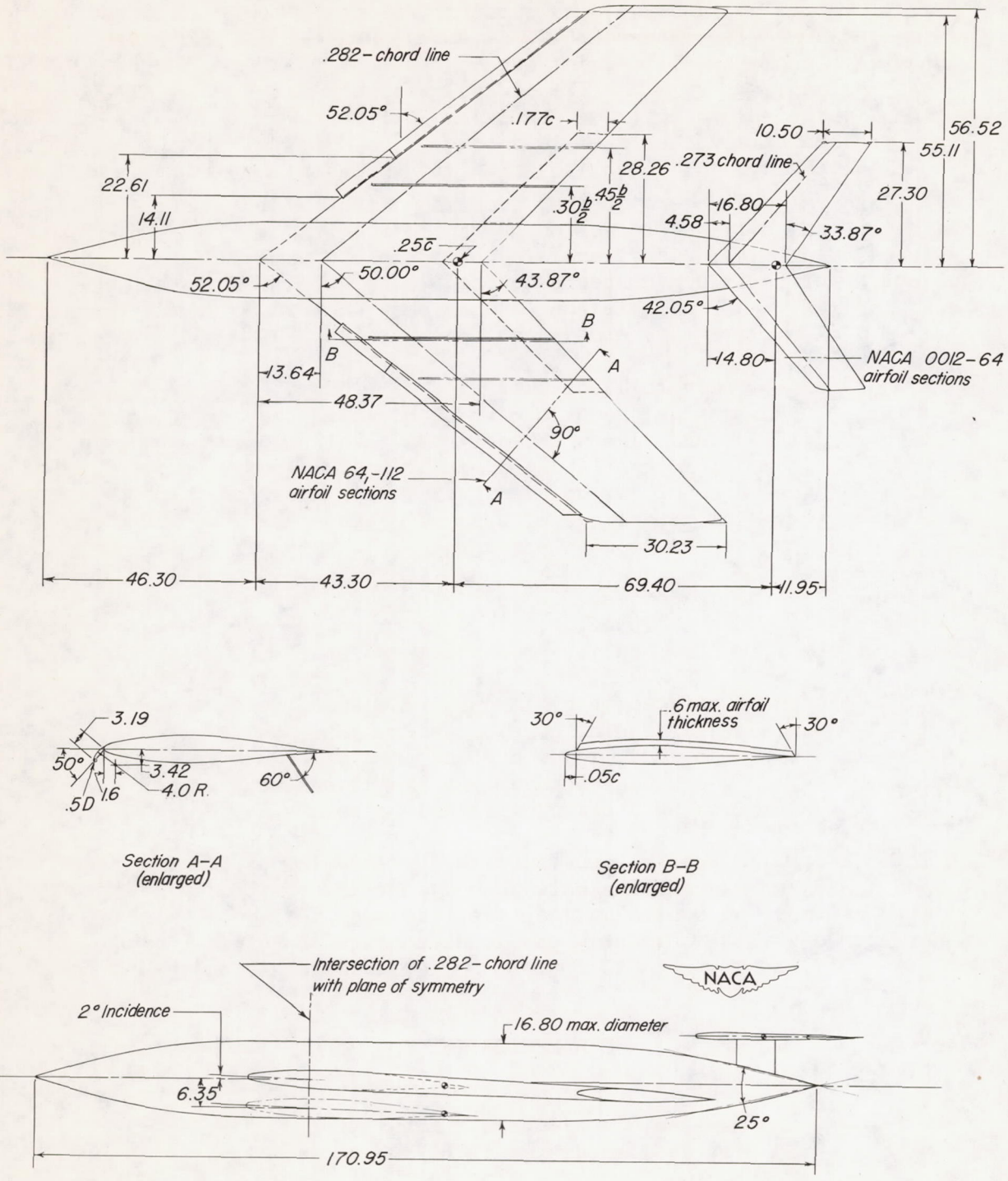

Figure 1.- Details of a 52° sweptback wing with fuselage and horizontal tail. Wing: aspect ratio = 2.88; taper ratio = 0.625; area = 4429 sq in.; $\bar{c}$ = 39.97 in. All dimensions in inches.

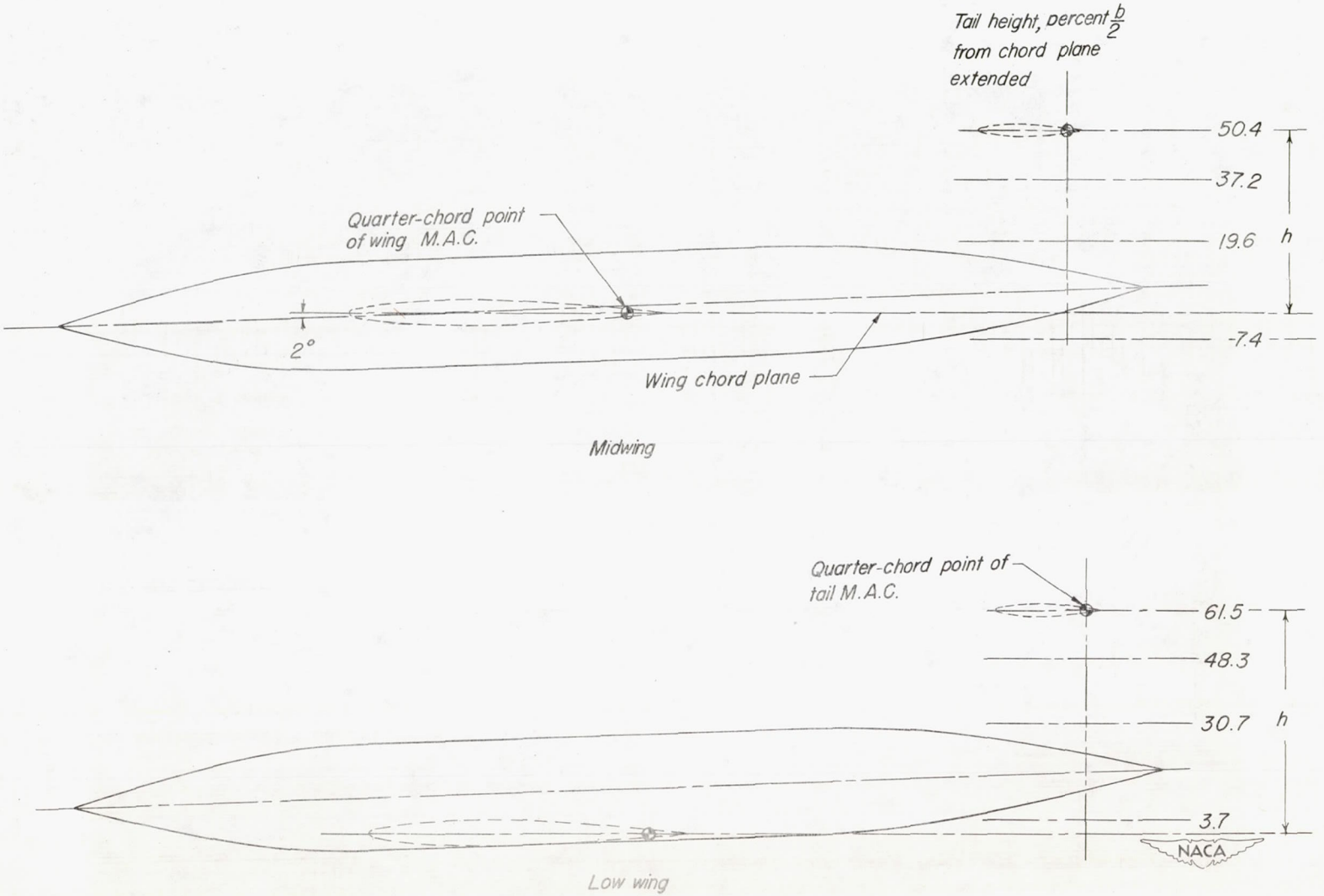

Figure 2.- Vertical position of horizontal tail with respect to chord plane of wing; mid-and low-wing-fuselage combination.

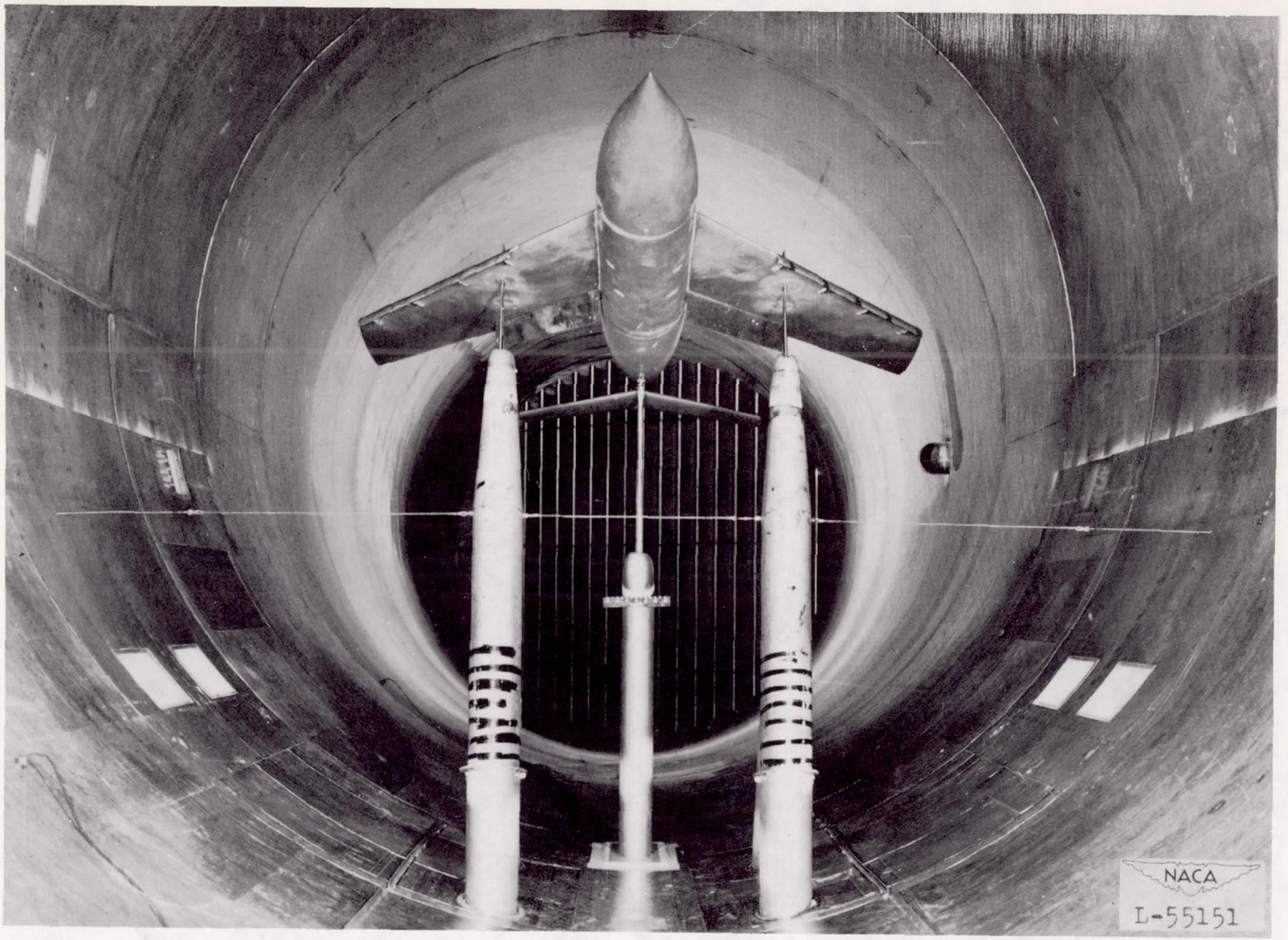

(a) Front view.

Figure 3.- A 52° sweptback wing-fuselage combination in the Langley 19-foot pressure tunnel.

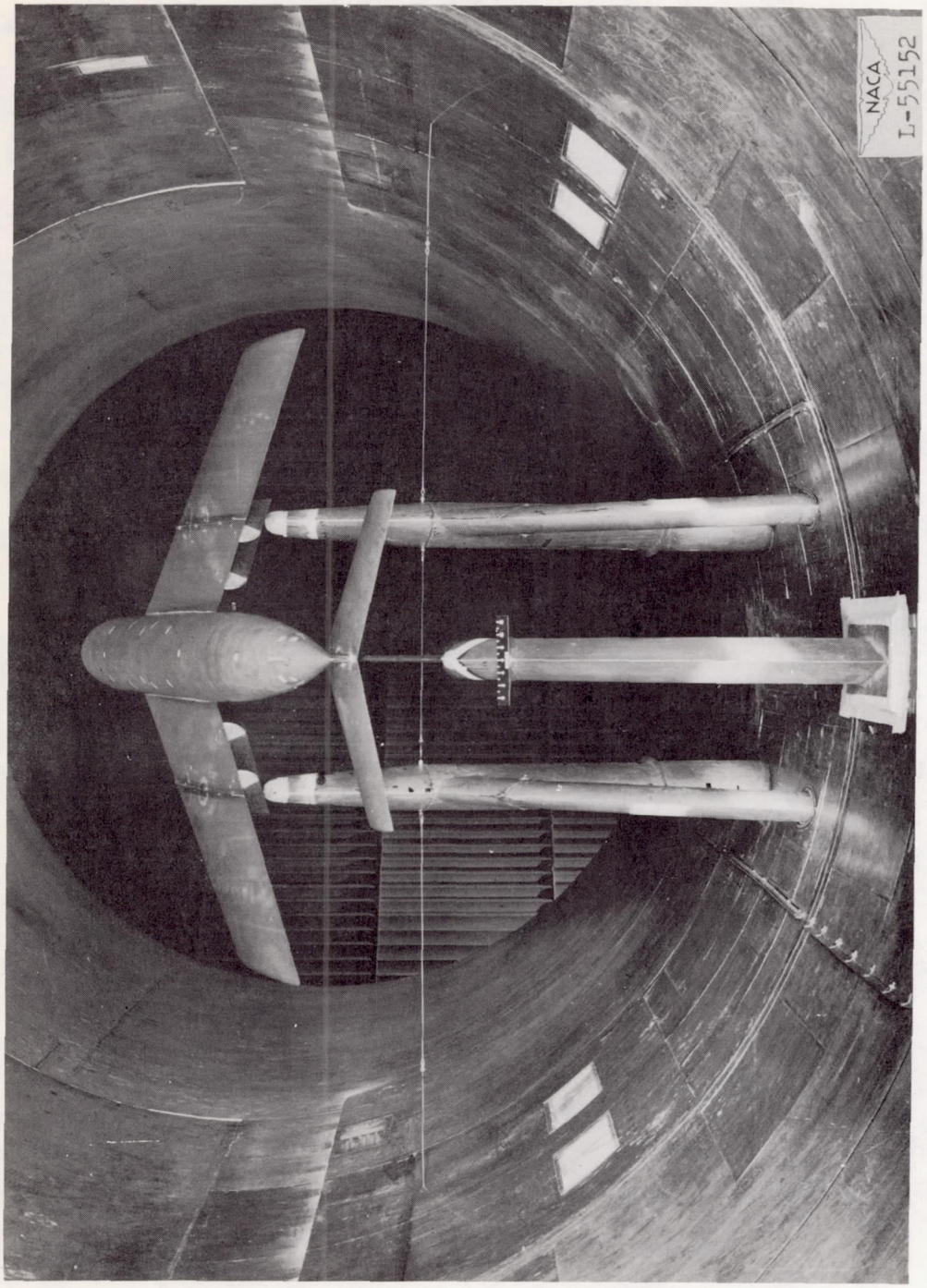

(b) Rear view.

Figure 3.- Concluded.

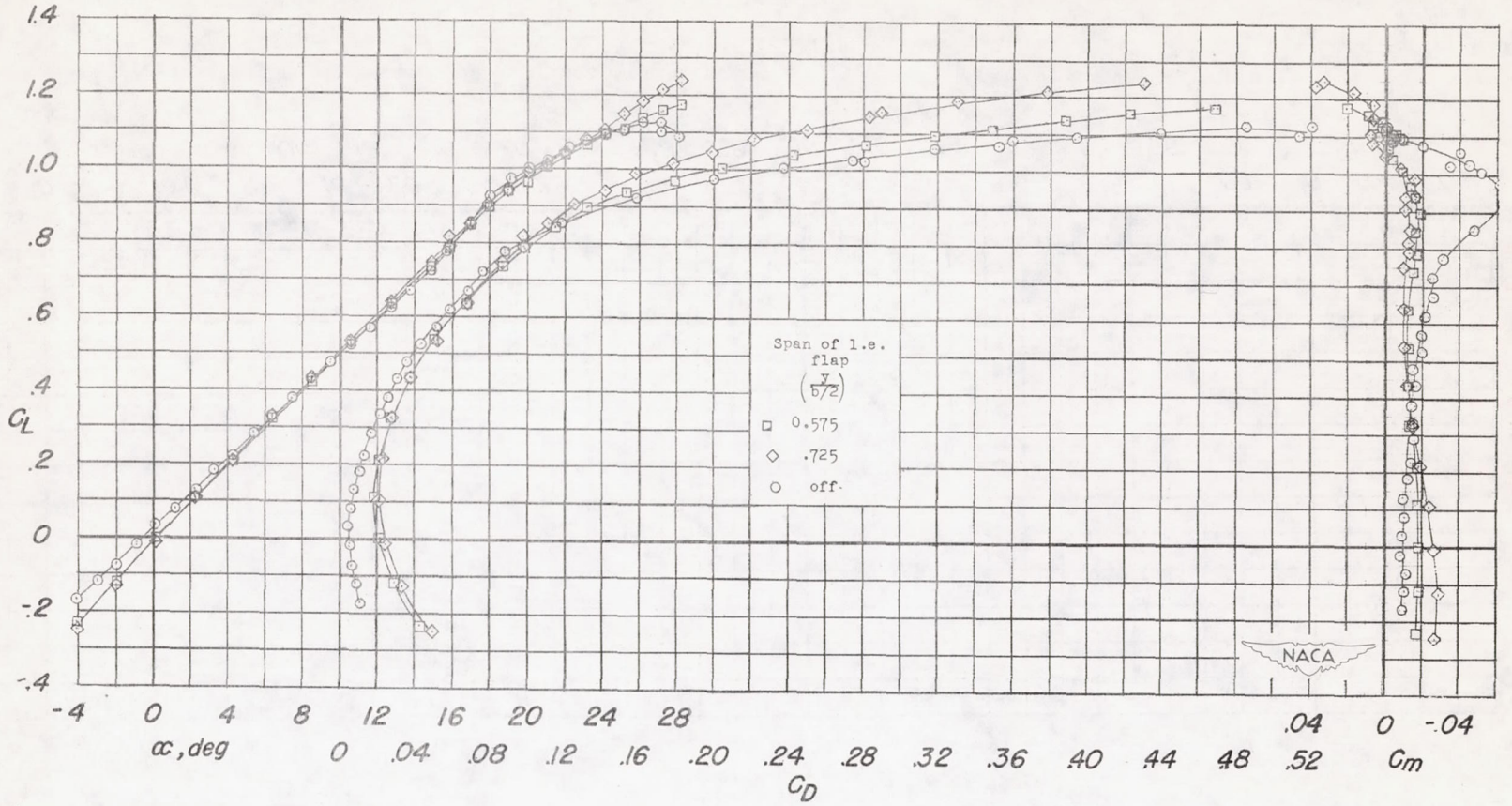

(a) Split flaps off.

Figure 4.- Aerodynamic characteristics of a 52° sweptback wing with and without leading-edges flaps.

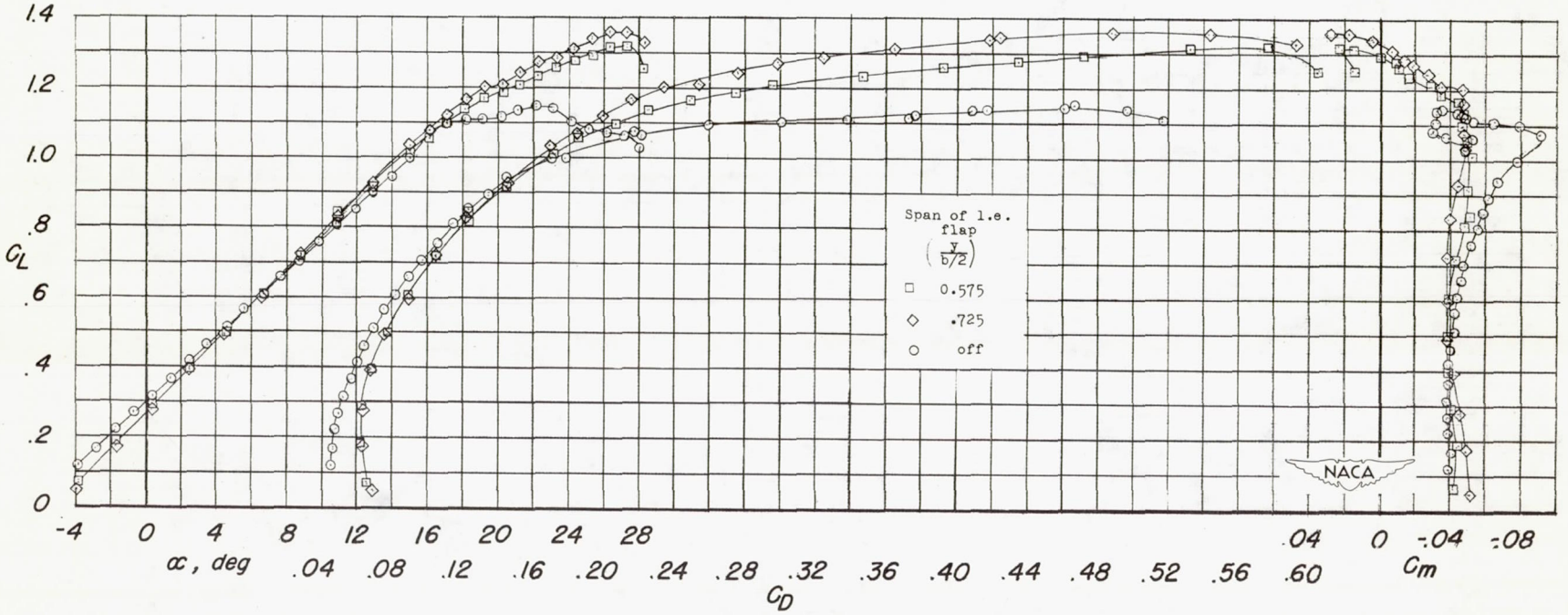

(b) Split flaps on.

Figure 4.- Concluded.

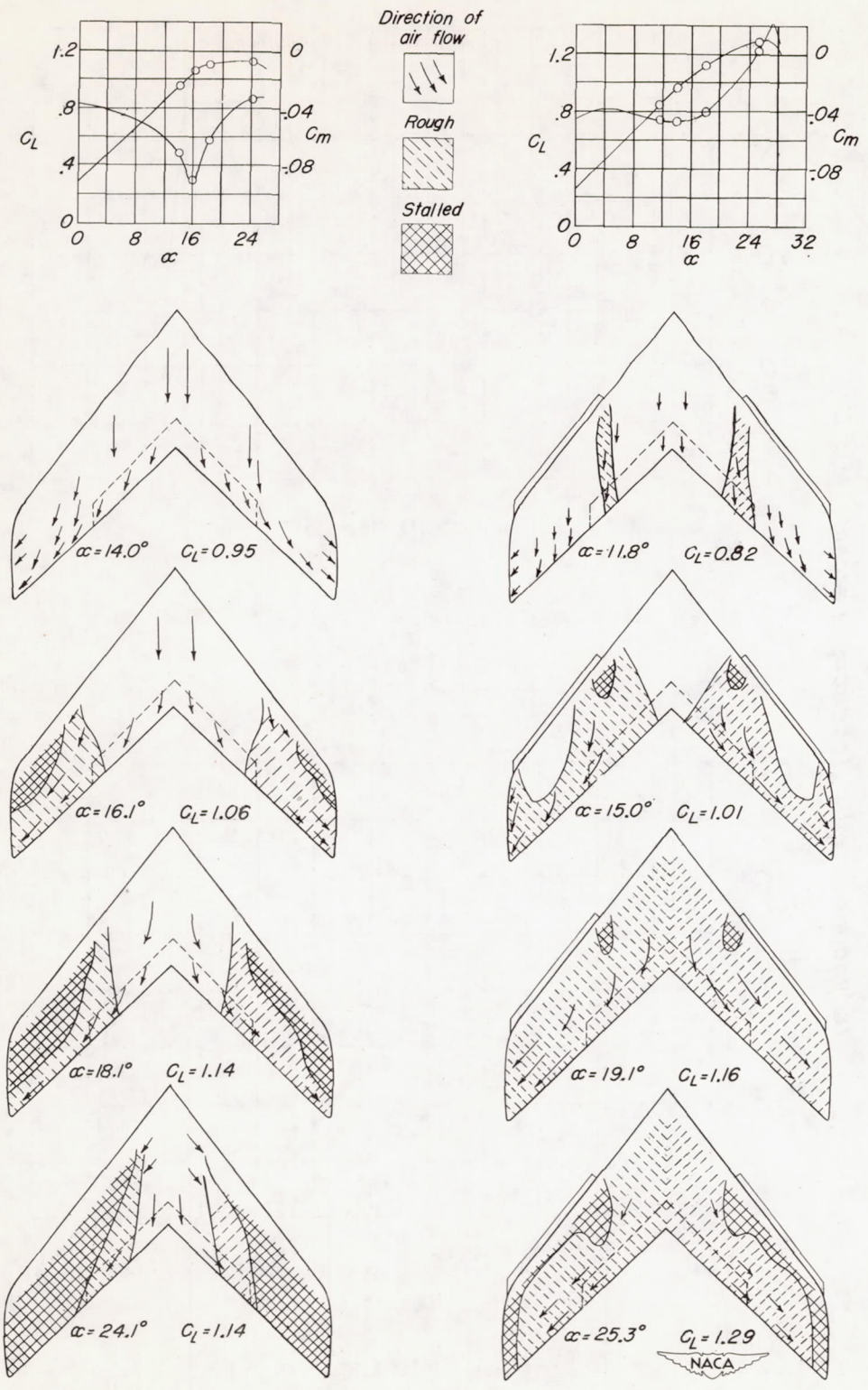

(a) Leading-edge flaps off (b) Leading-edge flaps on

Figure 5.- Stall studies of a 52° sweptback wing with and without $0.575\frac{b}{2}$ span leading-edge flaps; split flaps deflected.

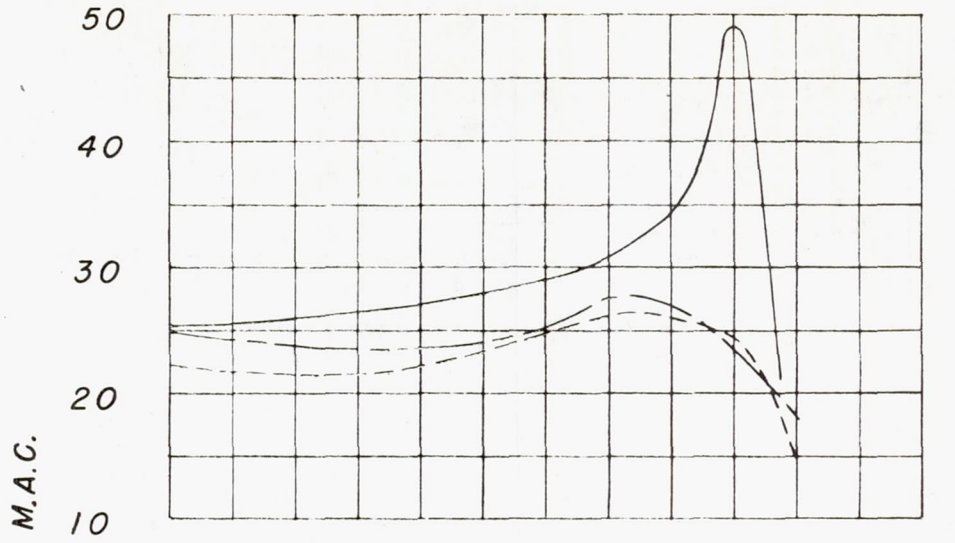

(a) Split flaps off.

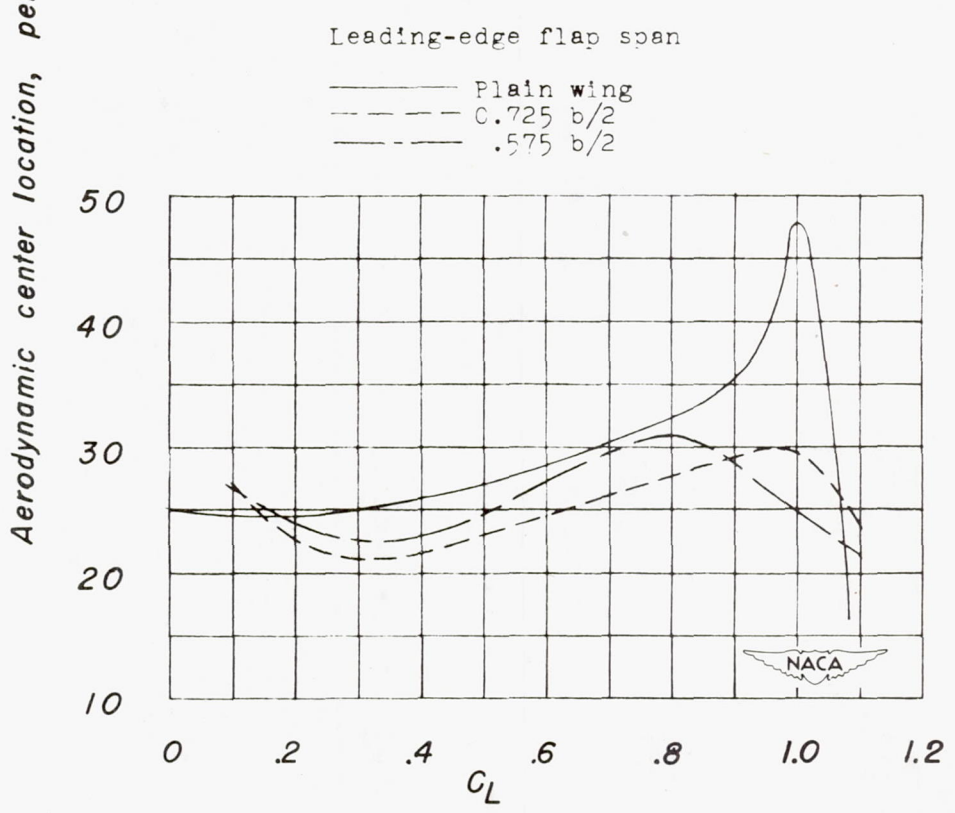

(b) Split flaps on.

Figure 6.- Variation of aerodynamic center with lift coefficient for a 52° sweptback wing with and without leading- and trailing-edge flaps.

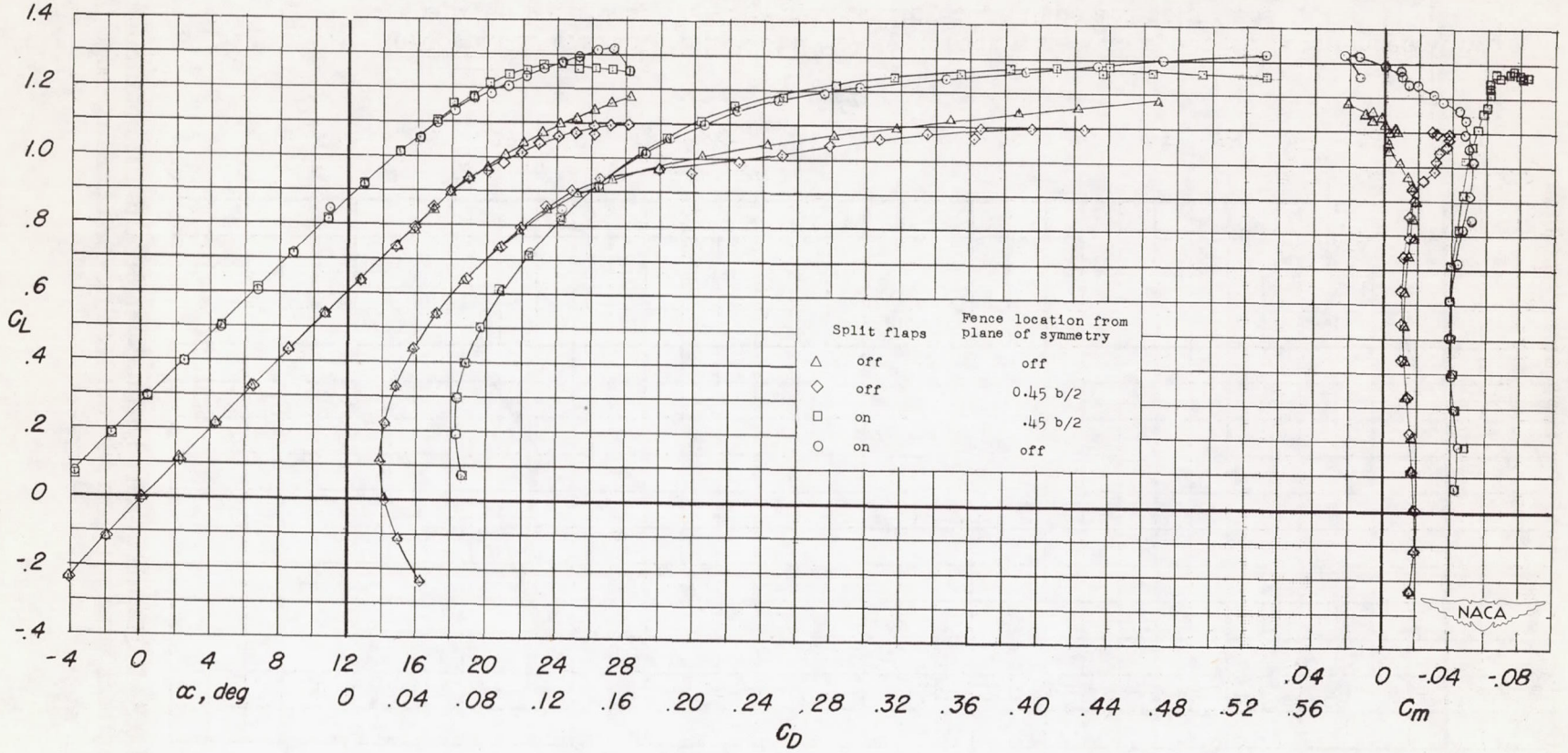

Figure 7.- The effect of split flaps and upper-surface fences on the aerodynamic characteristics of a 52° sweptback wing with $0.575\frac{b}{2}$ -span leading-edge flaps.

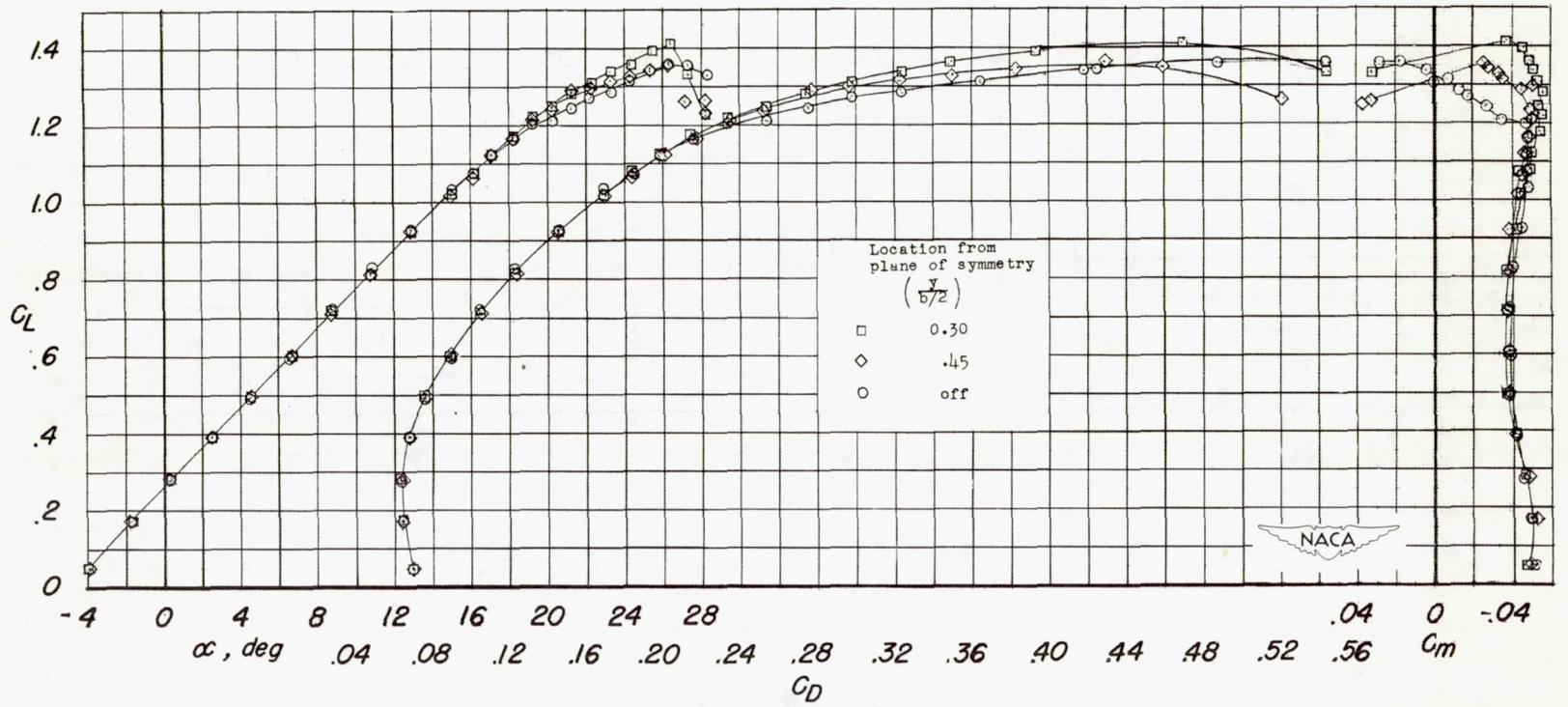

Figure 8.- Aerodynamic characteristics of a 52° sweptback wing with upper-surface fences at two spanwise locations. $0.725\frac{b}{2}$-span leading-edge flaps and split flaps on.

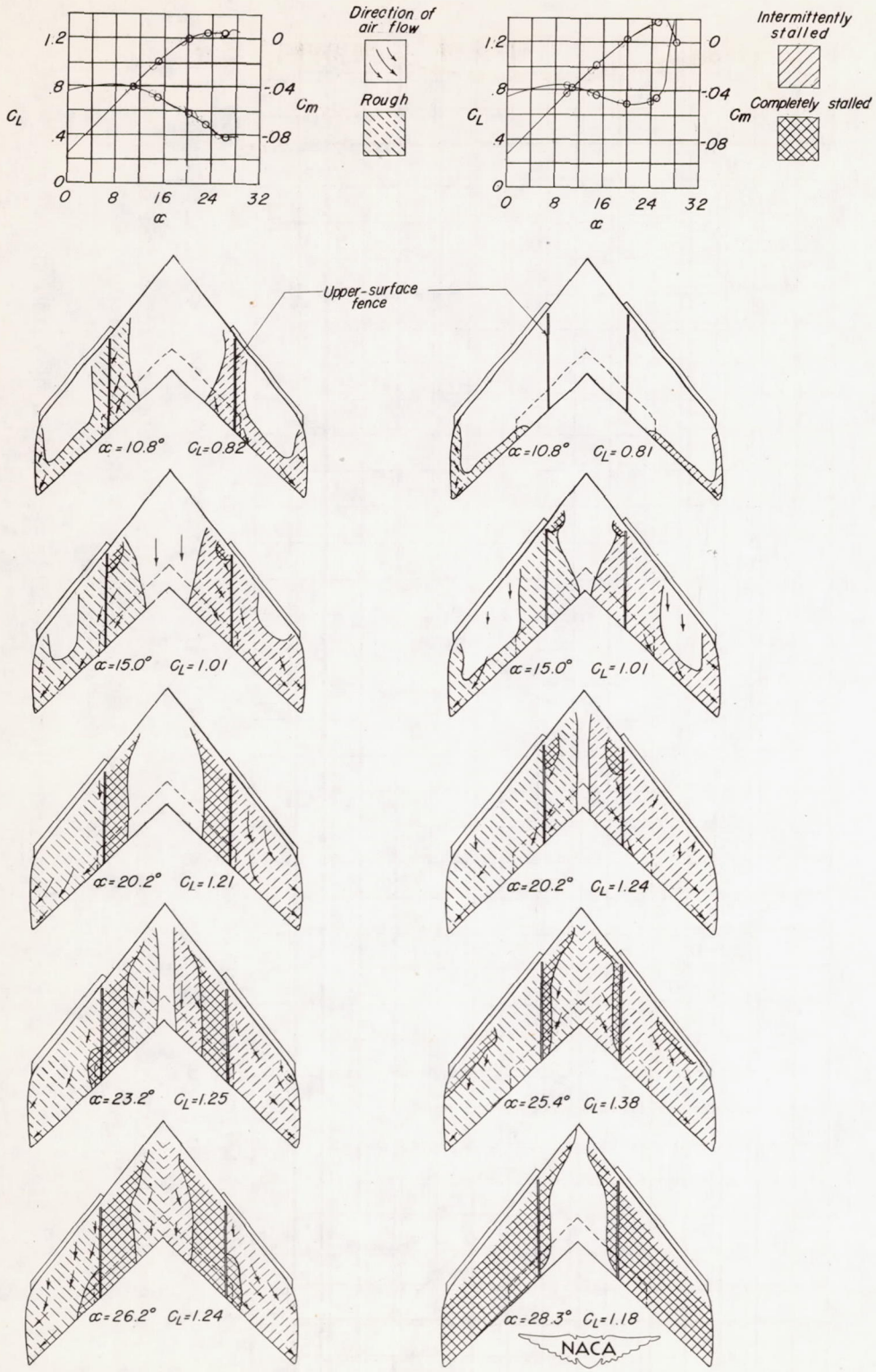

(a) $0.575\frac{b}{2}$ -span leading-edge flaps, fences at $0.45\frac{b}{2}$.

(b) $0.725\frac{b}{2}$ -span leading-edge flap, fences at $0.30\frac{b}{2}$.

Figure 9.- Stall studies of 52° sweptback wing in combination with leading-edge flaps and upper-surface fences.

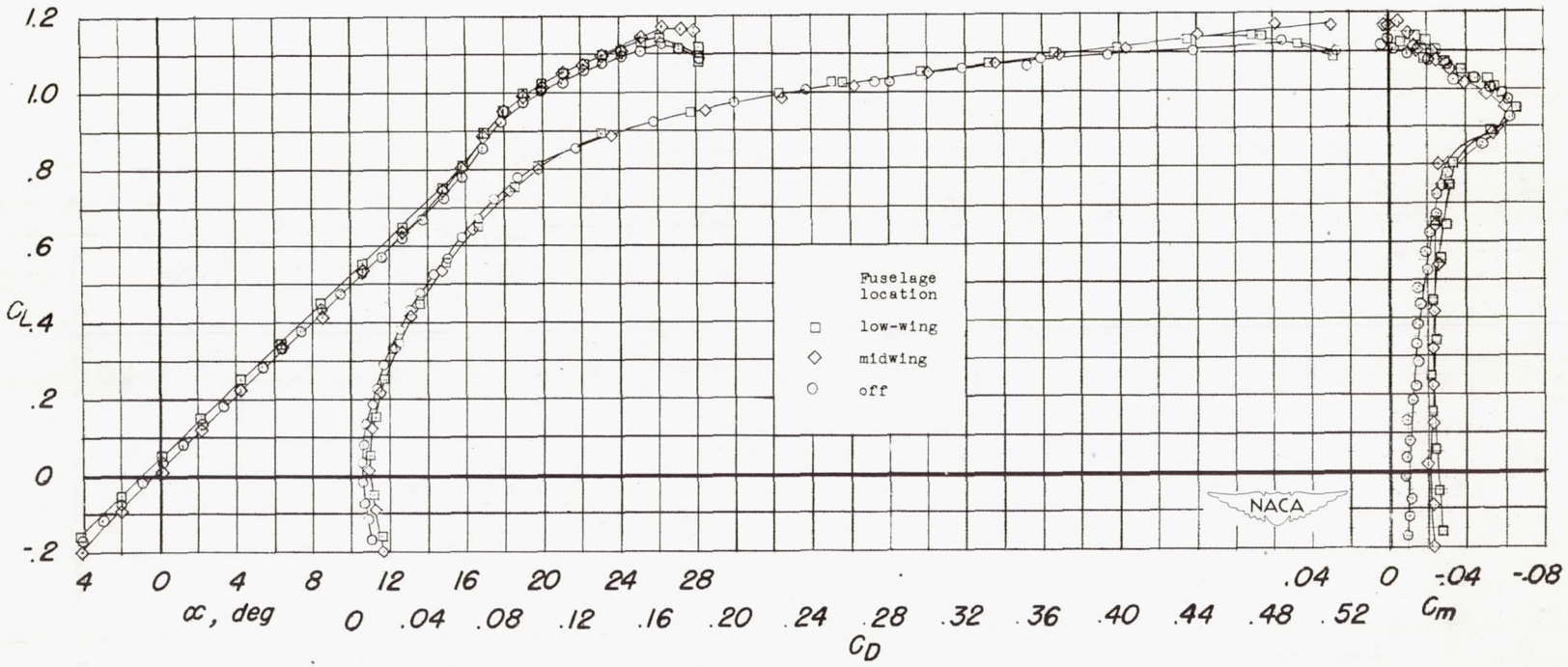

(a) Split flaps off.

Figure 10.- Aerodynamic characteristics of a 52° sweptback wing with fuselage on.

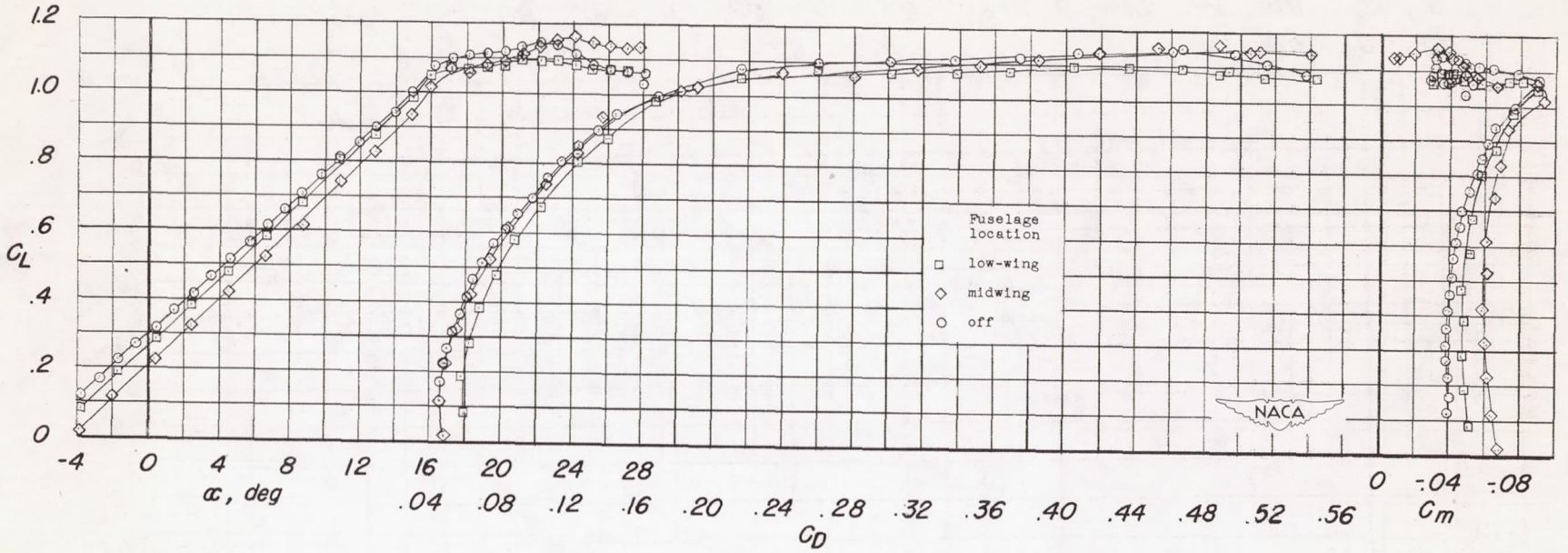

(b) Split flaps on.

Figure 10.- Concluded.

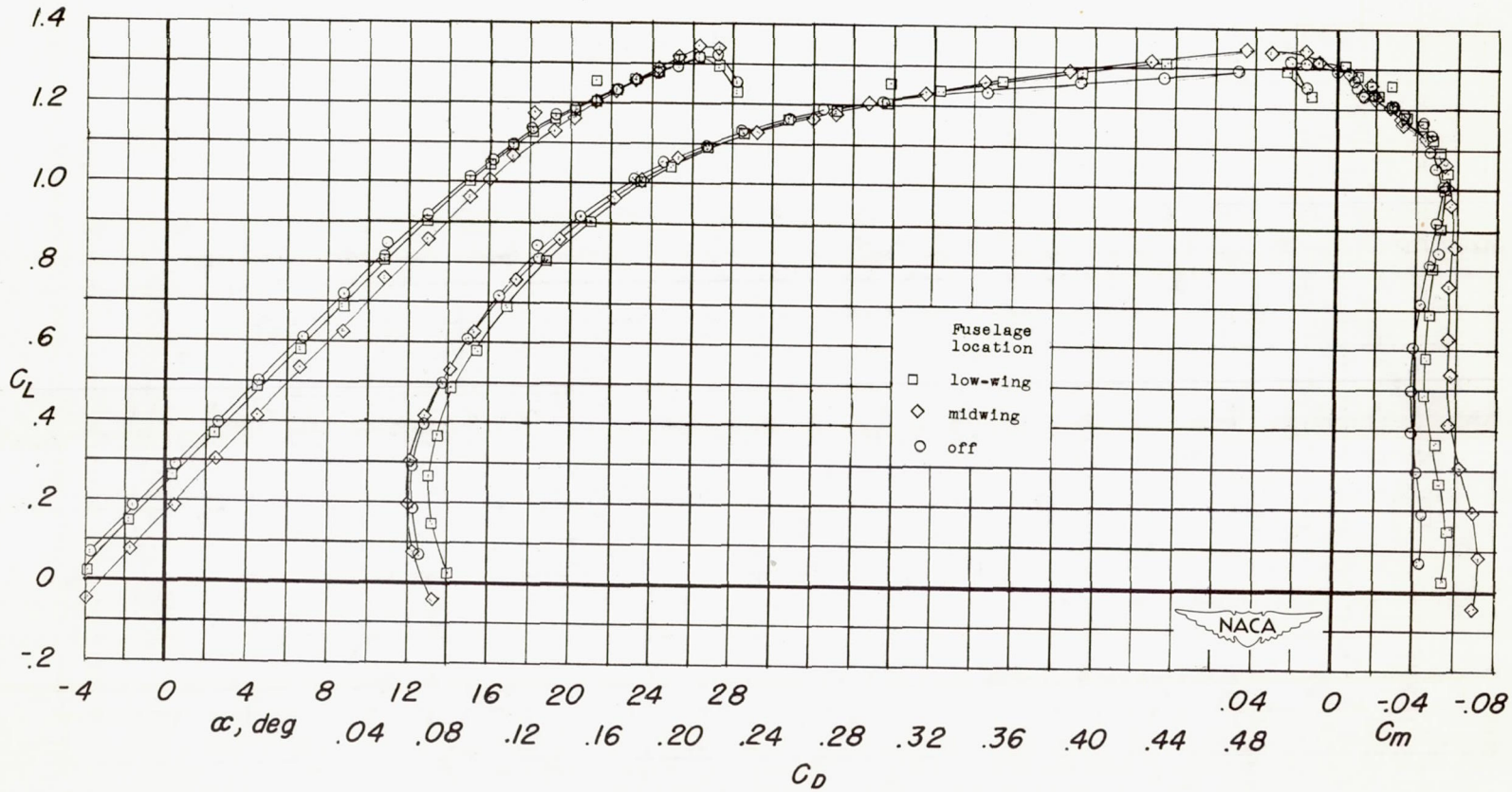

Figure 11.- Aerodynamic characteristics of a 52° sweptback wing with split flaps, $0.575\frac{b}{2}$-span leading-edge flaps, and fuselage.

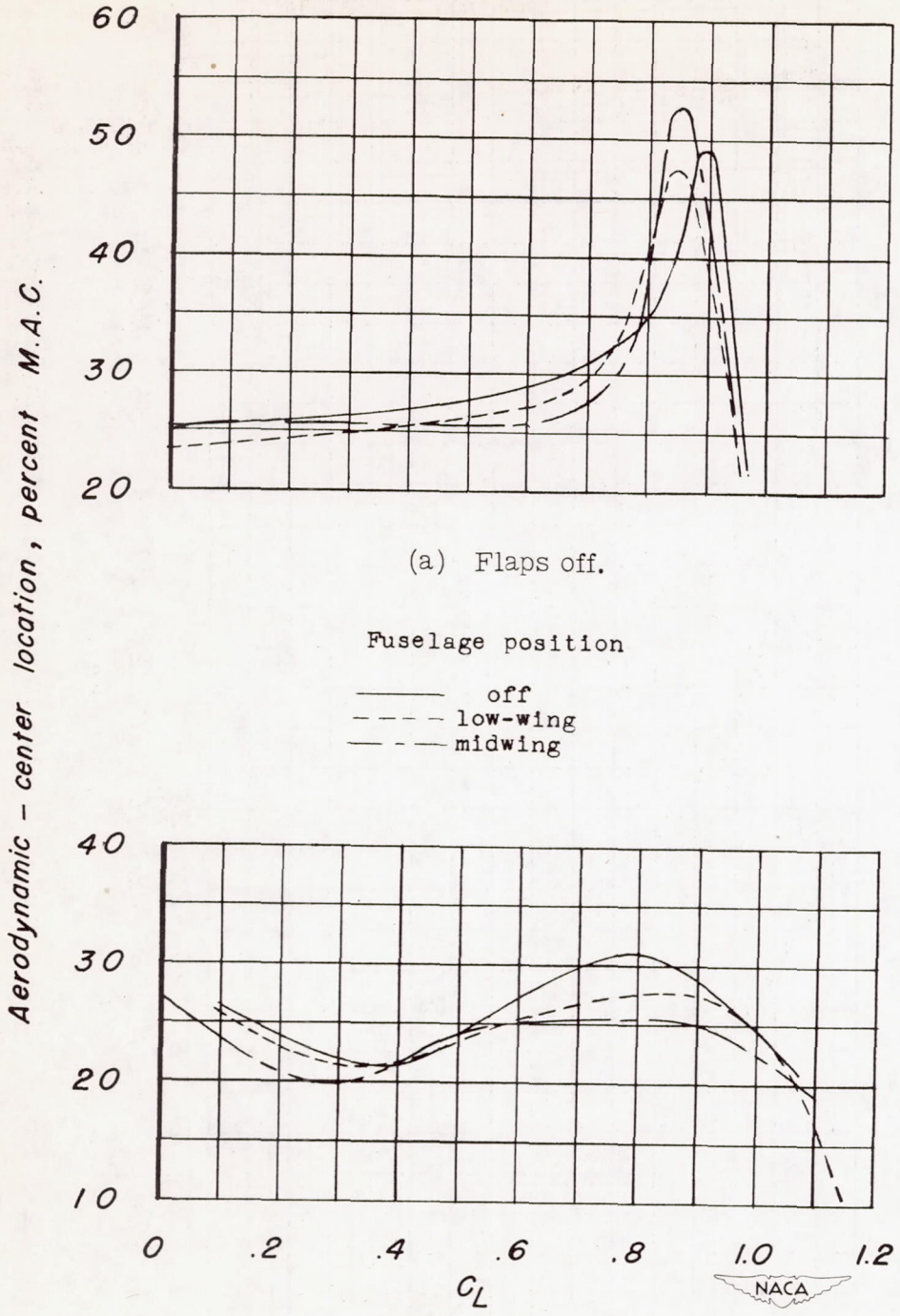

(a) Flaps off.

(b) Split and $0.575\frac{b}{2}$ —span leading-edge flaps.

Figure 12.- Variation of aerodynamic-center location with lift coefficient for a 52° sweptback wing with several fuselage positions.

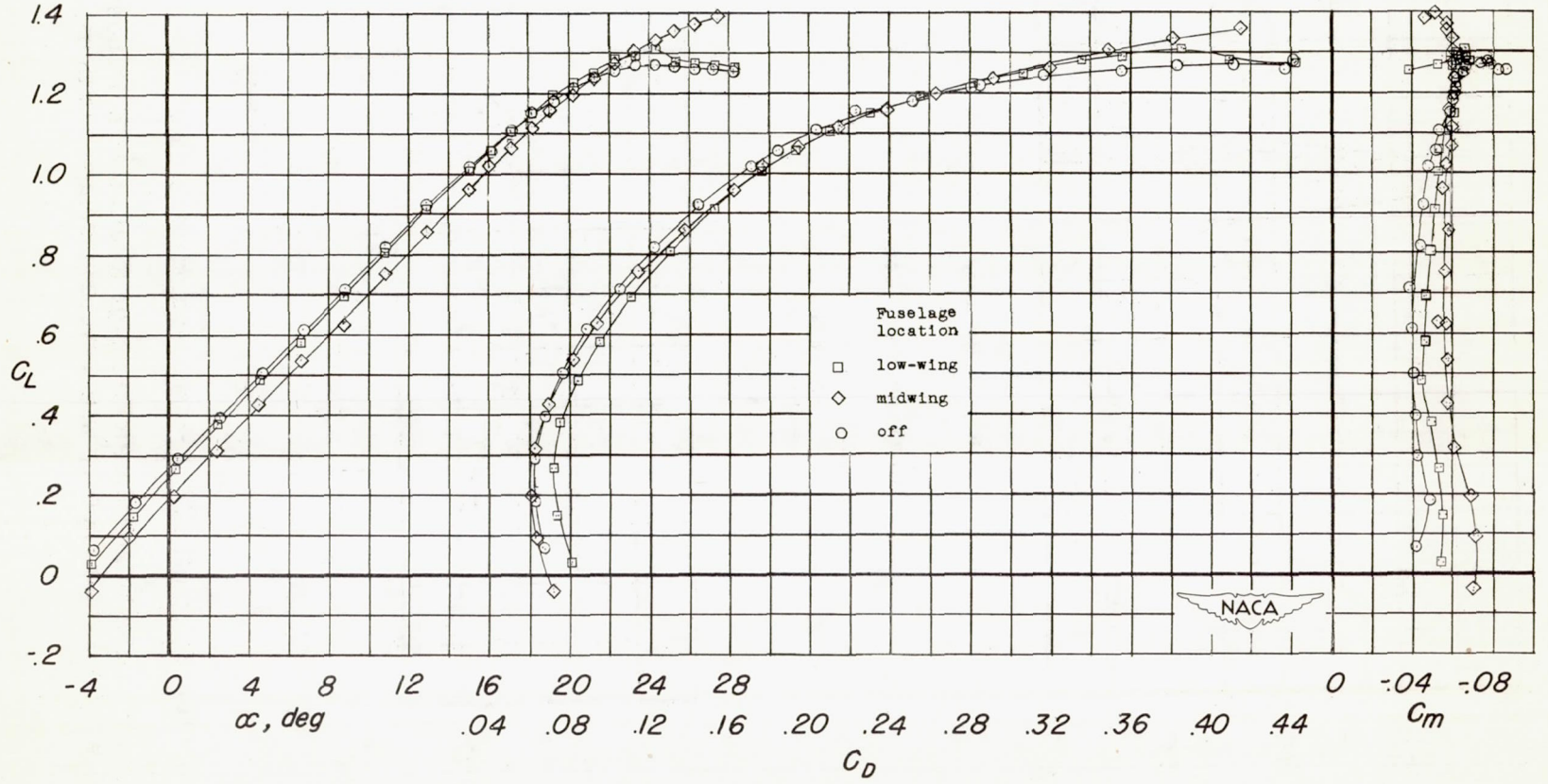

Figure 13.- Aerodynamic characteristics of a 52° sweptback wing with $0.575\frac{b}{2}$-span leading-edge flap, split flaps, upper-surface fences at $0.45\frac{b}{2}$, and fuselage.

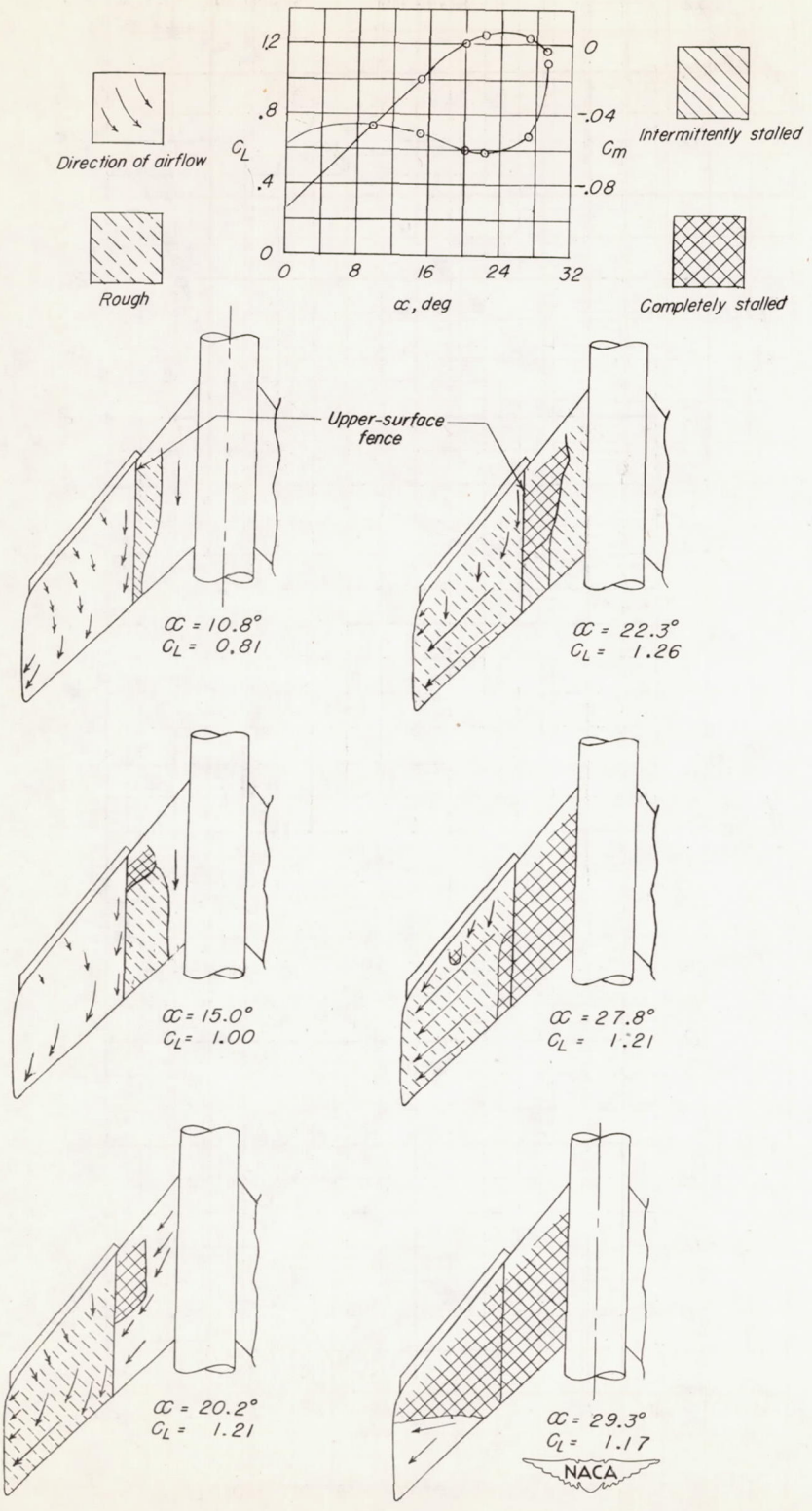

Figure 14.- Stall studies of a 52° sweptback wing with low-wing fuselage, $0.575\frac{b}{2}$-span leading-edge flaps, split flaps, and upper-surface fences.

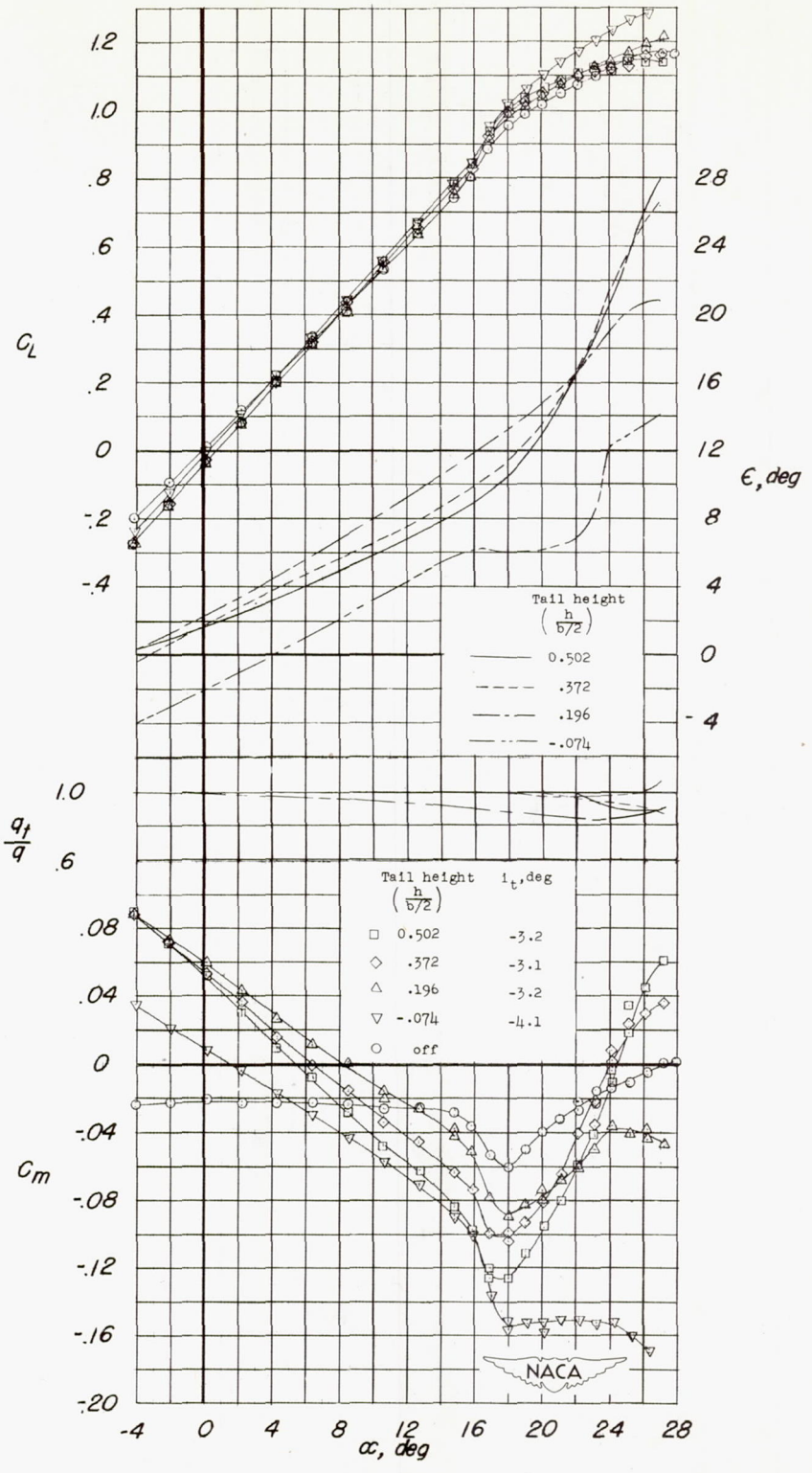

(a) Wing configuration - plain.

Figure 15.- Effect of a horizontal tail on the aerodynamic characteristics of a 52° sweptback wing with fuselage; midwing combination.

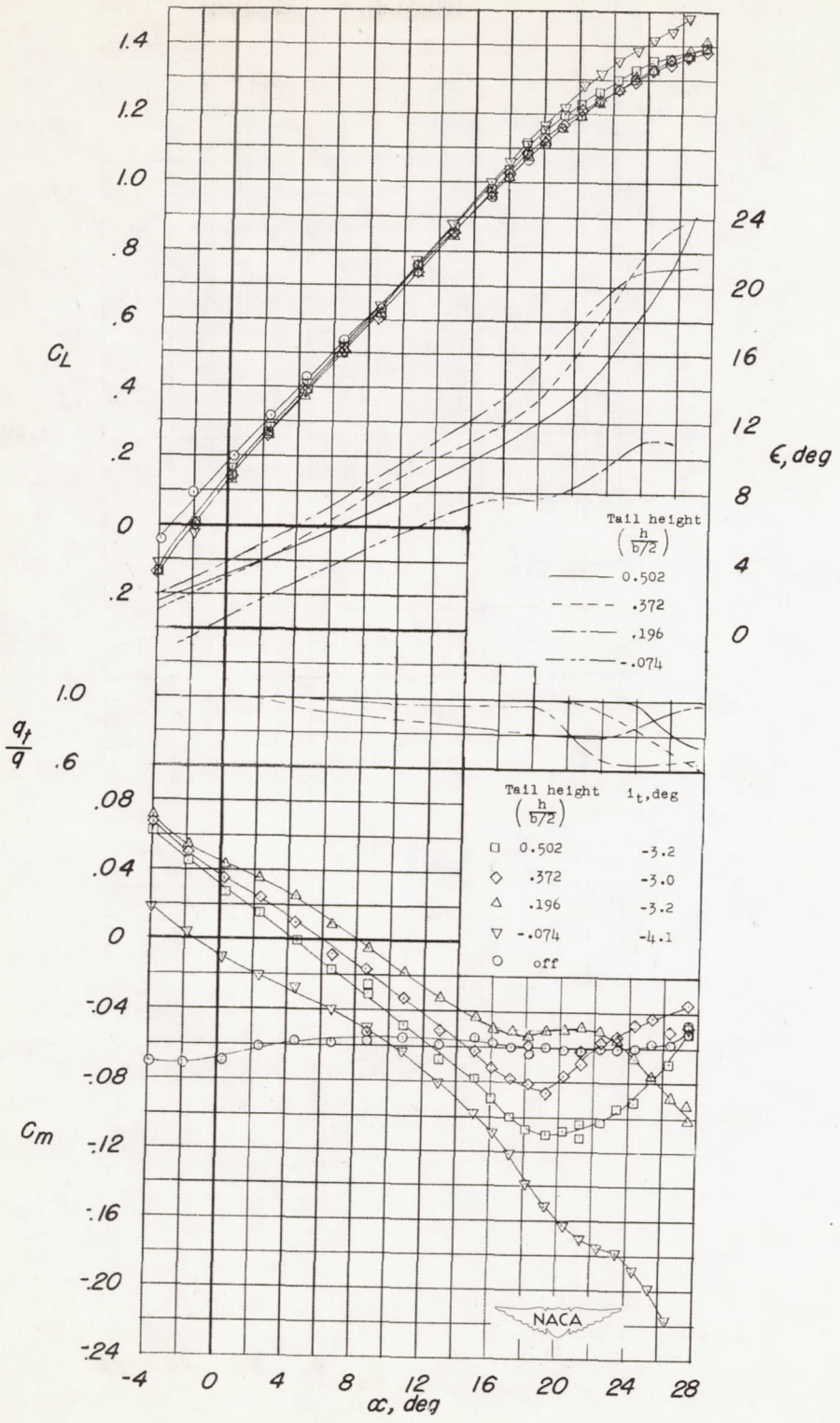

(b) Wing configuration - split flaps, $0.575\frac{b}{2}$-span leading-edge flaps, and fences at $0.45\frac{b}{2}$.

Figure 15.- Concluded.

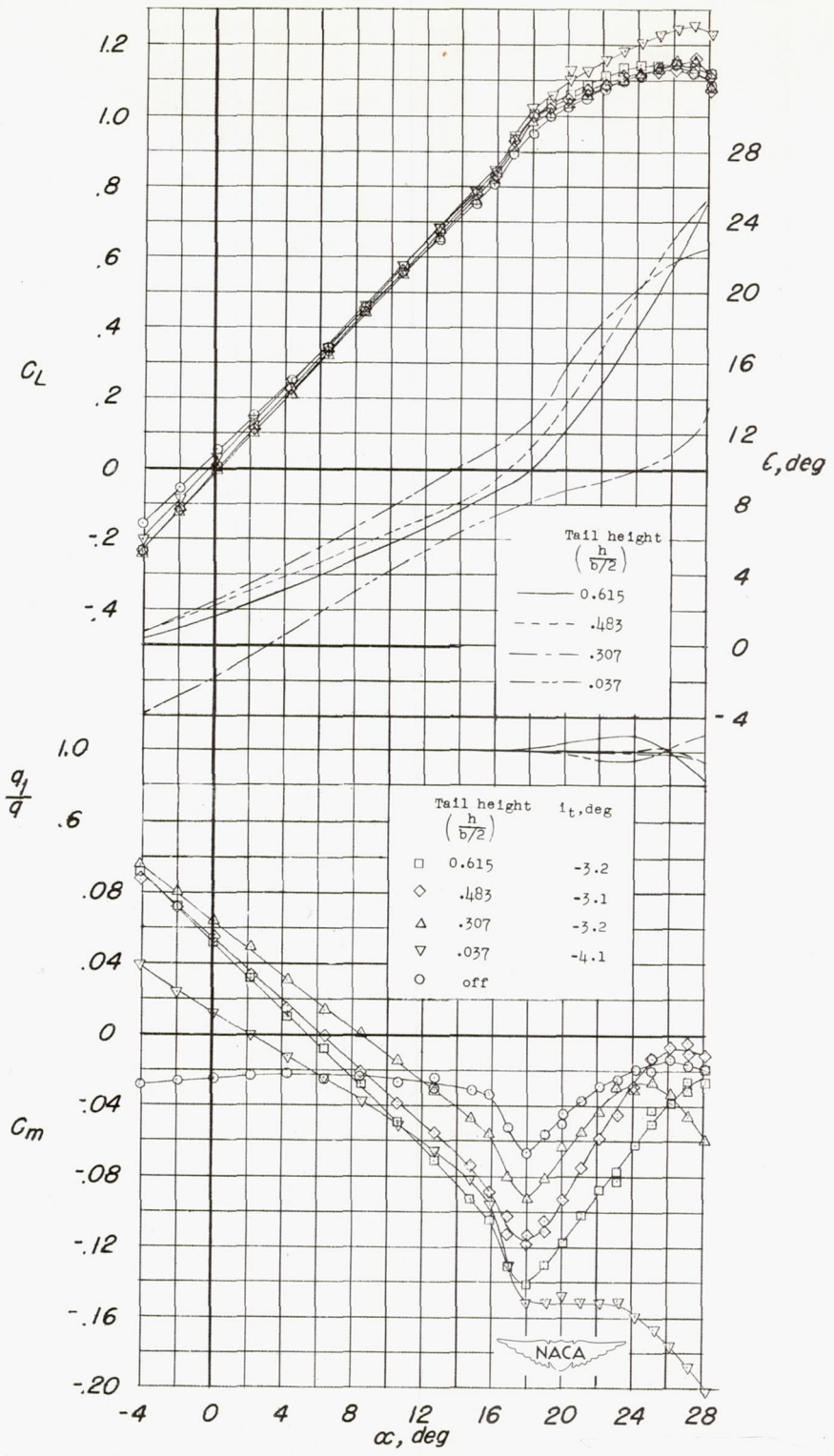

(a) Wing configuration - plain.

Figure 16.- Effect of a horizontal tail on the aerodynamic characteristics of a 52° sweptback wing with a fuselage; low-wing combination.

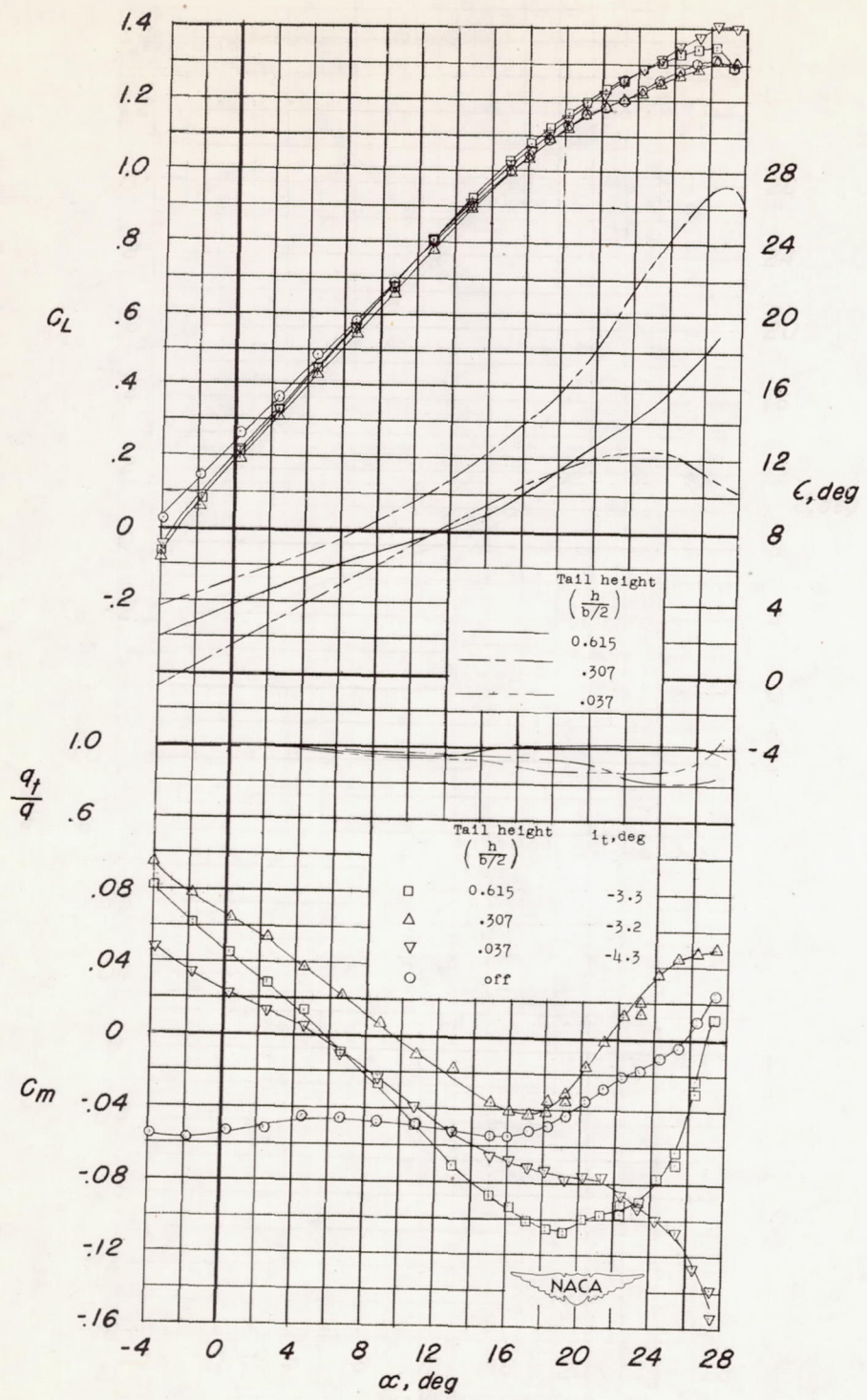

(b) Wing configuration - split flaps, and $0.575\frac{b}{2}$ -span leading-edge flaps.

Figure 16.- Continued.

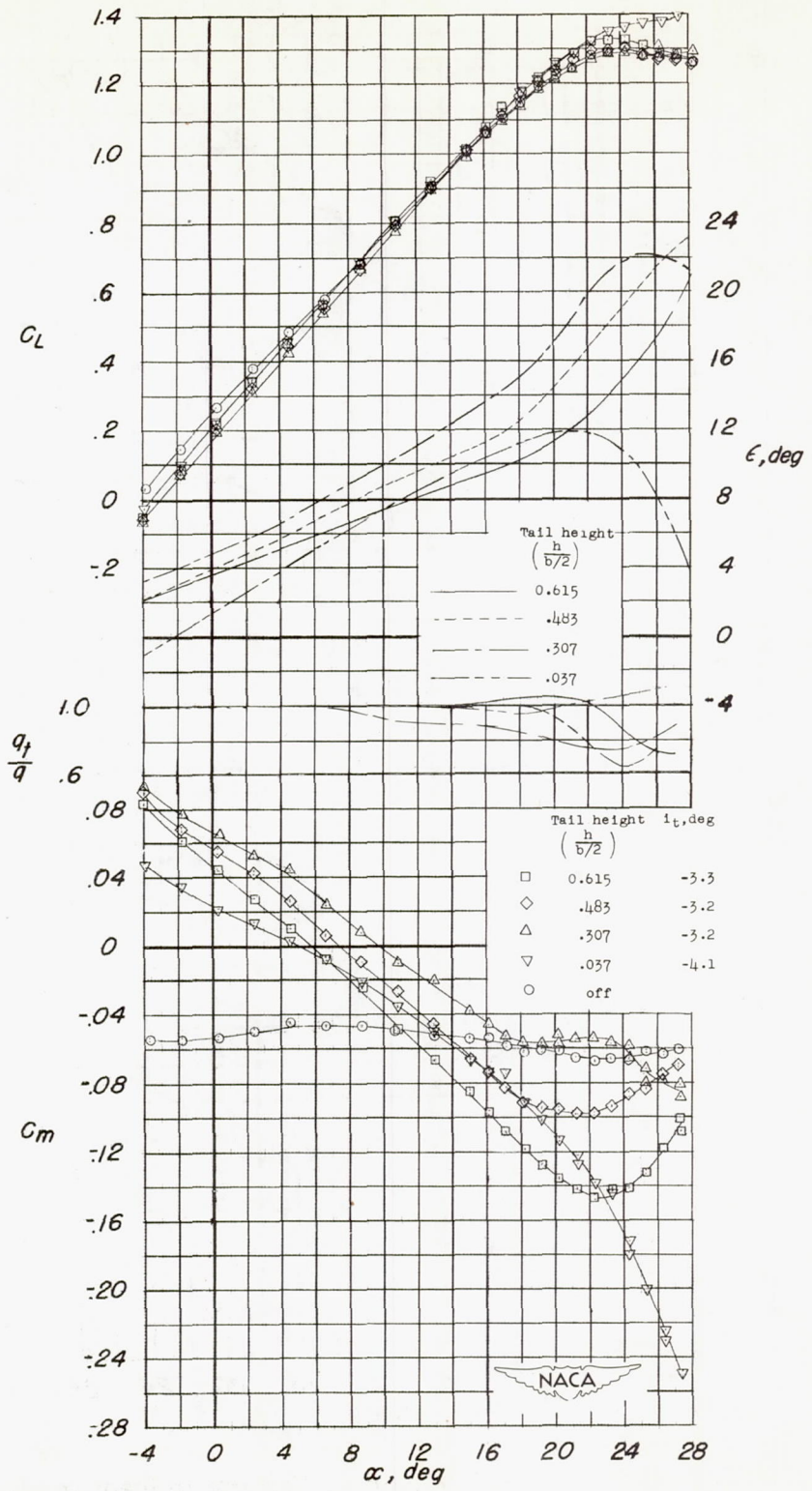

(c) Wing configuration - split flaps, $0.575\frac{b}{2}$ -span leading-edge flaps, and fences at $0.45\frac{b}{2}$.

Figure 16.- Concluded.

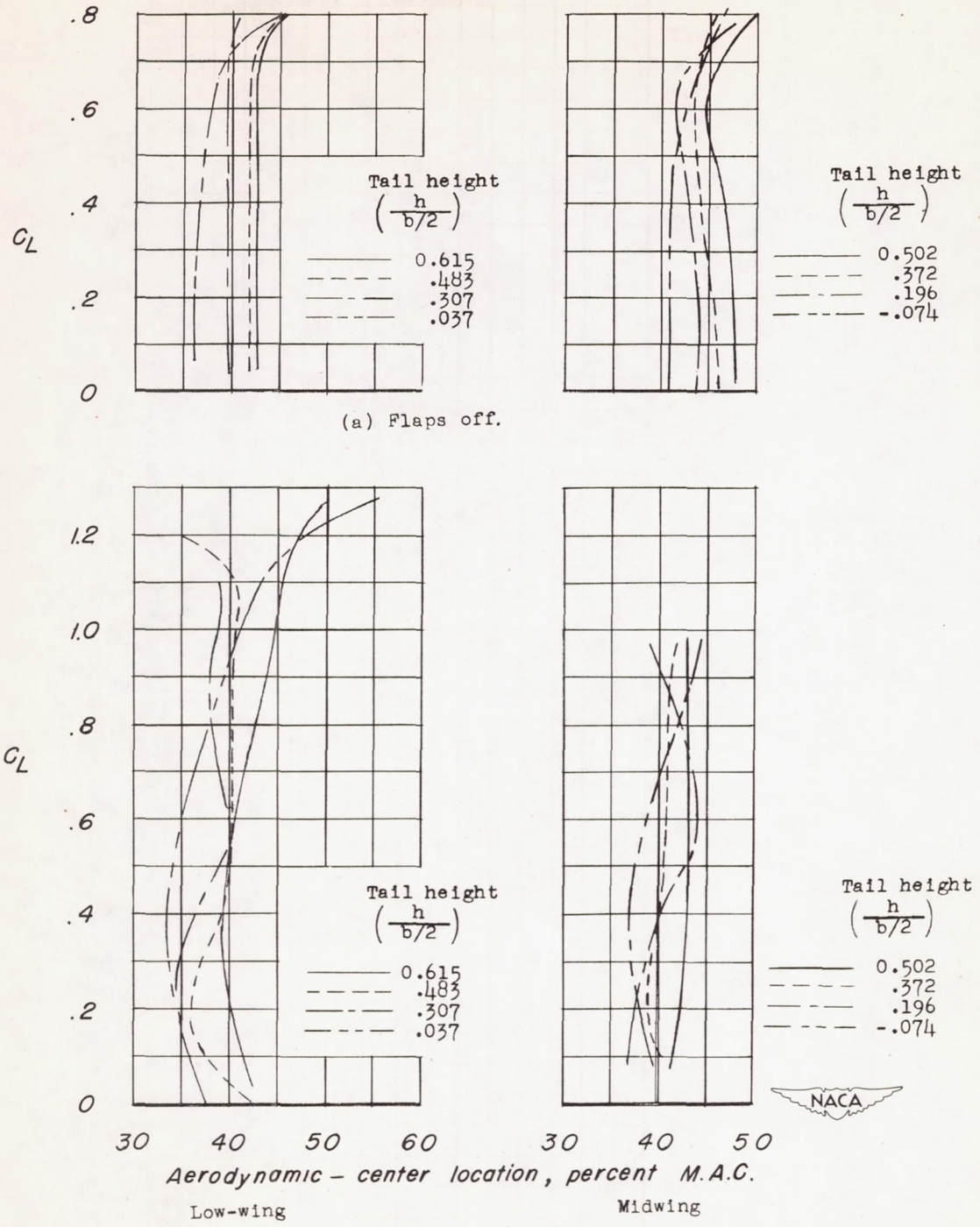

(b) Split and $0.575\frac{b}{2}$ -span leading-edge flaps and fences on.

Figure 17.- Variation of aerodynamic-center location with lift coefficient for a 52° sweptback wing-fuselage combination and horizontal tail.